Distributed Quantum Dense Coding With Nonclassical Routing

A Thesis

submitted to
Indian Institute of Science Education and Research Pune
in partial fulfillment of the requirements for the
BS-MS Dual Degree Program

by

Pratham H.P

Indian Institute of Science Education and Research Pune
Dr Homi Bhabha Road
Pashan, Pune 411008, India.

May, 2025

Supervisor: Prof. Ujjwal Sen

Certificate

This is to certify that this dissertation entitled **Distributed Quantum Dense Coding With Nonclassical Routing** towards the partial fulfilment of the BS-MS degree at the Indian Institute of Science Education and Research, Pune represents study/work carried out by Pratham H.P at Harish-Chandra Research Institute, Prayagraj (Allahabad) under the supervision of Prof. Ujjwal Sen, Professor and Director, Department of Physics, during the academic year 2024 - 2025.

Prof. Ujjwal Sen

Committee
Prof. Ujjwal Sen
Prof. T. S. Mahesh

I dedicate this thesis to my family for their endless love and support throughout my pursuit of education.

Declaration

I hereby declare that the matter embodied in the report entitled **Distributed Quantum Dense Coding With Nonclassical Routing** are the results of the work carried out by me at the Department of Physics, Harish-Chandra Research Institute, Prayagraj (Allahabad), under the supervision of Prof. Ujjwal Sen and the same has not been submitted elsewhere for any other degree. Whenever others contribute, every effort is made to indicate this clearly, with due reference to the literature and acknowledgement of collaborative research and discussions.

Pratham H.P
20201158

List of Publications

This thesis is based on a pre-print that was written during the period of my MS research project.

- Pratham Hullamballi, Aparajita Bhattacharyya, and Ujjwal Sen, "Distributed Quantum Dense Coding Enhanced With Non-classical Routing" arxiv: 2503.16122

Acknowledgement

I want to express my deepest gratitude to my supervisor, Professor Ujjwal Sen, for his support and guidance over the past year; his unwavering support has been instrumental throughout this thesis. I truly enjoyed and cherished our discussions, learning a great deal from them on the foundations of quantum theory, communication, cryptography, and life in general. The way he has shaped my thinking as a researcher will stay with me throughout my career and beyond. I am also deeply indebted to Professor T. S. Mahesh for his mentorship throughout my time at IISER. I sincerely appreciate his willingness to take me under his mentorship in 2022 when I was exploring summer projects, and I thank him for introducing me to the field of quantum computing and information theory. I extend my thanks to Professor M. S. Santhanam for his mentorship and for introducing me to variational quantum algorithms. I would also like to thank Aparajita and Debarupa for their mentorship during my time at HRI.

Beyond academics, I am profoundly grateful to my parents and grandparents for their understanding, continuous support and encouragement throughout this journey. I thank them for wholeheartedly supporting me in the pursuit of my interests.

Finally, I would like to thank my friends at IISER, HRI, and from school for the many wonderful memories, stimulating discussions, and moments of joy that have enriched my journey.

Abstract

In entanglement-assisted communication theory, it is well-known that pre-shared entanglement between a sender and receiver facilitates decoding a maximum of two bits of information by sending just one qubit. This is commonly referred to as quantum dense coding. In the recent decade, several works have shown that using a control system to create additional resources like coherent control and indefinite causal order has provided advantages in communication protocols. Inspired by these, we propose a distributed dense coding protocol that uses a control system to superpose two dense coding processes, allowing us to simultaneously and coherently encode and non-classically route the sender's single-qubit system to two receiver labs. We find that dense coding with coherently controlled encoding and routing performs better than the standard dense coding protocol in both global and one-way LOCC decoding strategies employed by receiver labs in weak entanglement regimes and with noisy mixed states.

Contents

List of Figures

Chapter 1

Introduction

The development of communication protocols has traditionally been rooted in classical information theory, where data is encoded and transmitted using classical bits. However, the advent of quantum mechanics has fundamentally altered the foundations of information science by providing us with the quantum extension of Shannon's classical information theory, arguably a more general framework for communication theory [51]. By utilising non-classical resources like entanglement and superposition, communication protocols offer capabilities far beyond classical limits [17].

Any communication scheme, quantum or classical, for sending classical information, involves three major steps - (1) encoding of classical information into a physical system, (2) sending of the physical system through a physical channel, and (3) decoding of classical information from the received physical system. Communication protocols that involve encoding and decoding classical information through quantum states shared between distant parties are broadly referred to as quantum-assisted classical communication or classical communication through quantum channels [53, 6]. Here, the physical system is a quantum system, and the physical channel is a quantum channel. In a seminal paper from Holevo [28], a hard bound on the amount of classical information extractable from a quantum system was derived. It proved that the amount of classical information that can be sent via d-dimensional quantum system is at most $\log_2 d$ bits, therefore implying one cannot decode more than n bits of information from n qubits. The first instance of a quantum-assisted classical communication protocol giving an advantage over existing classical protocols was introduced by Bennett and Wiesner in 1992 [5], called quantum dense coding, where they used pre-shared entan-

glement between the sender and receiver as a resource to communicate 2 bits of information by transmitting only a single qubit, seemingly "surpassing" the Holevo bound. The trick lies in pre-sharing a Bell state, thereby increasing the dimension of the quantum system and, consequently, the value of the Holevo bound. Further works have generalised dense coding protocol with mixed states of arbitrary dimension [36, 7], multiple senders and up to 2 receivers [7, 8], and noisy channels [16, 45]. To characterise the maximum potential of a dense coding protocol for a given state, the concept of dense coding capacity (DC capacity) was introduced. DC capacity proved to be helpful at characterising the role of entanglement in dense coding and explicitly showed that bound-entangled states are not useful for dense coding [7]. Quantum dense coding has been experimentally realised in many quantum hardware setups, including atomic systems [43], photonic qubits [37, 4, 33, 52, 30], optical modes [35, 32], and nuclear magnetic resonance (NMR) [20, 49].

In recent years, there has been a growing interest in using a coherent quantum system [2, 21] to do mainly two things - (1) put the causal ordering of any two quantum channels into a superposition in an approach known as quantum `SWITCH` [12, 19], rendering the causal order of the channel 'indefinite' [24] and (2) to coherently control quantum channels themselves, usually referred to as channel multiplexing or a 'quantum half-`SWITCH`' [1]. The latter approach was first introduced in error filtration [22]. These approaches show classical and quantum capacity enhancement when used in communication protocols [13, 1, 19]. It was discovered that one could transmit non-zero information using a quantum state passing through either a quantum `SWITCH` or quantum half-`SWITCH` of two completely depolarising channels [1, 19]. In a complete surprise, perfect quantum communication with two completely depolarising channels using quantum `SWITCH` was proven to be possible [11]. Further resource-theoretic studies on the superposition of quantum trajectories and their role in communication protocols have also been investigated [34, 48]. Experimental attempts using interferometric setups have been made to explore communication advantages using superposition of trajectories [39, 41, 42, 25, 23, 50, 26, 47, 40]. Inspired by the possibility of using a coherent quantum system as a control to superpose two situations, we will use a coherent quantum system to superpose two dense coding scenarios, allowing coherently controlled encoding and non-classical routing of the sender's system to two receiver labs.

This thesis delves into leveraging a coherent quantum system to create a superposition of two physical processes and using it to enhance quantum dense coding protocol. Specifically, we design a distributed dense coding protocol that uses a control quantum system to encode

and non-classically route the sender's quantum system to two receiver labs. We investigate the DC capacity when the two receiver labs are together and find a lower bound to the "local" DC capacity when they are distant but can do one-way classical communication. We also extend it to the distributed case involving an arbitrary number of receiver labs. We find that our protocol performs better than the standard dense coding protocol in both global and one-way LOCC decoding scenarios in low entanglement regimes and with mixed states.

Chapter 2 introduces some basic but necessary terminologies and concepts from classical and quantum Shannon theory for formalising general classical communication protocols with quantum systems as information carriers. A brief dive into quantum measurements and accessible information in global and LOCC decoding scenarios is provided.

Chapter 3 goes into explicit details of a quantum-assisted classical communication protocol known as quantum dense coding or super-dense coding. We explain the idea of dense coding with a single sender and a single receiver and extend to multiple senders and up to two receivers. We analytically derive standard dense coding capacities for various states.

In Chapter 4, we describe our variant of the dense coding protocol where we use a coherent quantum system to encode and non-classically route the sender's system to two different receiver labs. We explain our approaches to calculating the dense coding capacity when the labs employ global measurement strategies and locally accessible information when labs employ a one-shot, one-way LOCC decoding strategy.

In Chapter 5, we conclude our thesis by summarising our findings.

Chapter 2

Background and Preliminaries

Before delving into the thesis, it would be helpful to know some basic and essential concepts from classical and quantum Shannon theory. This will allow us to introduce concretely the general quantum dense-coding protocol and other relevant concepts. A considerable chunk of classical and quantum Shannon theory is presented here from [51].

2.1 Classical Shannon Theory

2.1.1 Shannon Entropy

Let X be a random variable whose realisations x are *letters* in an *alphabet* $\mathcal{X}$. Let $p_X(x)$ denote the probability density function of X; that is, $p_X(x)$ is the probability that a realisation x occurs. If we were to formally define 'information', we would want it to be a measure of surprise. We would be more surprised if an event with very little probability happened and would, therefore, gain more information. In comparison, we gain less information about a high-probability event happening as we would be expecting it anyway, and its occurrence would be less surprising. Motivated by this, the information content $i(x)$ of a realisation x can be defined as:

$$i(x) \equiv -\log(p_X(x)) \tag{2.1}$$

This definition captures the idea that information is additive in that learning two independent events would mean we have more information and that higher probability events have a lower surprise element and, therefore, lower information content. The negative sign ensures positivity as $0 \leq p_X(x) \leq 1$. To capture the general notion of information content in a

random variable X, the entropy $H(X)$, also referred to as Shannon entropy, is introduced and defined to be the expected information content of a random variable X,

$$H(X) \equiv \mathbb{E}_X\{i(X)\} = -\sum_{x\in\mathcal{X}} p_X(x)\log\left(p_X(x)\right) \tag{2.2}$$

where we adopt the convention $0\log 0 = 0$. This convention is justified via limit argument because $\lim_{x\to 0} x\log(1/x) = 0$. Shannon entropy has the following info-theoretic interpretation: Alice and Bob were supposed to do an experiment together, but due to some issues, Bob was not available. So, Alice proceeds to perform some random experiment that happens to select a realisation x of a random variable X associated with probability density $p_X(x)$. Bob, who happens to not be present during the experiment, has not learnt the outcome of the experiment. In this scenario, an interpretation of the Shannon entropy $H(X)$ is that it quantifies Bob's uncertainty about the random variable X before learning it. Under this interpretation, the expected information Bob gains after learning the outcome of the random experiment is $H(X)$. In fact, it can be rigorously proved that for Bob to be able to decode a compressed message, Alice needs to send Bob bits at the rate $H(X)$. This is given by Shannon's noiseless coding theorem.

2.1.2 Conditional Shannon Entropy

Suppose Alice and Bob possess discrete random variables X and Y, respectively. If X and Y are not statistically independent, we say they share correlations and that Bob has access to "side-information" about X in the form of Y. Defining $i(x|y) \equiv -\log(p_{X|Y}(x|y))$, the conditional entropy $p_{X,Y}(x,y)$ is given by,

$$H(X|Y) \equiv \mathbb{E}_{X,Y}\{i(X|Y)\} = -\sum_{x,y} p_{X,Y}(x,y)\log(p_{X|Y}(x|y)) \tag{2.3}$$

where $p_{X,Y}(x,y)$ is the joint probability distribution of X and Y, and $H(X|Y)$ is the amount of uncertainty that Bob has about X given that he already possesses Y. This intuitively implies that $H(X) \geq H(X|Y)$, a result that can be rigorously proven, and its equality implies that X and Y are independent random variables. What this result tells us is that conditioning does not increase entropy; uncertainty can only be reduced by learning something.

2.1.3 Joint Shannon Entropy

If Bob knows neither X nor Y, then the joint entropy $H(X,Y)$ describes his uncertainty, and is given by,

$$H(X,Y) \equiv \mathbb{E}_{X,Y}\{i(X,Y)\} = -\sum_{x,y} p_{X,Y}(x,y)\log(p_{X,Y}(x,y)) \tag{2.4}$$

The relation between joint entropy, conditional entropy and marginal entropy is given $H(X,Y) = H(X) + H(Y|X) = H(Y) + H(X|Y)$.

2.1.4 Mutual Information

If Alice and Bob possess discrete random variables X and Y, respectively, the entropic measure quantifying their shared knowledge is given by mutual information $I(X;Y)$ defined as

$$I(X;Y) \equiv H(X) - H(X|Y) \tag{2.5}$$

The expression above has the following interpretation meaning: Before Bob had access to Y, his uncertainty about X is $H(X)$, and once he possesses Y, the uncertainty reduces to $H(X|Y)$; therefore, the amount by which the uncertainty is reduced, $H(X) - H(X|Y)$, is the common/mutual information between Alice and Bob. It is natural to expect $I(X;Y) = I(Y;X)$ from the above argument, so the mutual information is symmetric. Mutual information is guaranteed to be non-negative, i.e. $I(X;Y) = H(X) - H(X|Y) \geq 0$ because $H(X) \geq H(X|Y)$.

2.1.5 Conditional Mutual Information

We now wish to quantify the common information between two random variables X and Y when some side information exists in the form of a random variable Z. The entropic quantity useful in this scenario is referred to as conditional mutual information. If X, Y and Z are discrete random variables, the conditional mutual information is defined as

$$I(X;Y|Z) \equiv H(Y|Z) - H(Y|X,Z) = H(X|Z) - H(X|Y,Z) \tag{2.6}$$

In fact, it is easy to see that

$$I(X;Y|Z) = \sum_z p_Z(z) I(X:Y|Z=z) \tag{2.7}$$

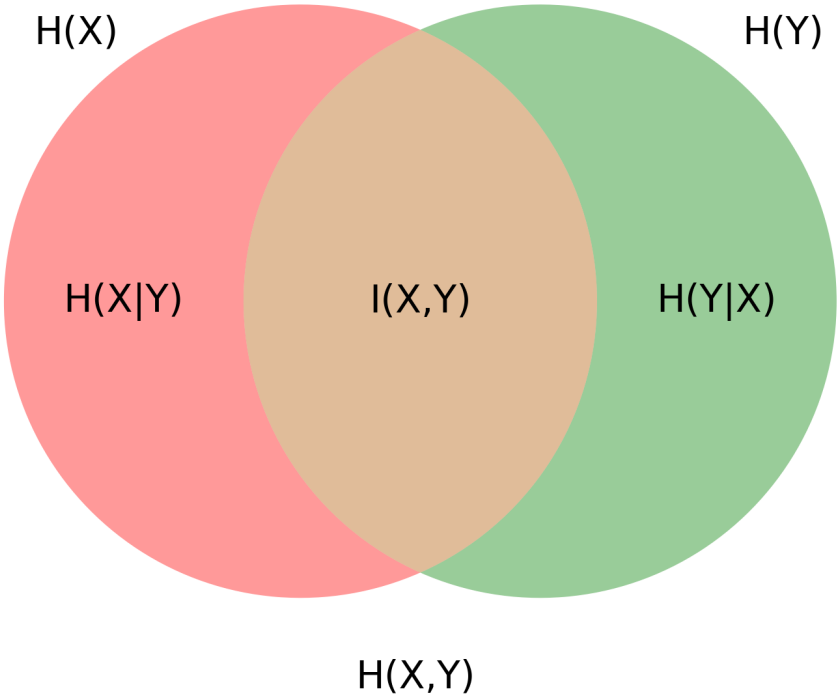

Figure 2.1: Classical Shannon entropic quantities can be equivalently represented by Venn diagrams. The first circle (coloured peach and brown) represents $H(X)$, the second circle (coloured green and brown) represents $H(Y)$, and the intersection represents the mutual information $I(X;Y)$. Removing the intersection (coloured brown) from each circle gives conditional entropies $H(X|Y)$ and $H(Y|X)$. The total Venn diagram (peach, brown and green) represents the joint entropy $H(X,Y)$.

where $I(X : Y|Z = z)$ is a mutual information with respect to joint probability density $p_{X,Y|Z}(x,y|z)$ and the marginal probability densities $p_{X|Z}(x|z)$ and $p_{Y|Z}(y|z)$.

Using this, one can derive a 'chain" rule for mutual information, taking the following form

$$I(X_1,\cdots,X_n;Y) = I(X_1;Y) + I(X_2;Y|X_1) + \cdots + I(X_n;Y|X_1,\cdots,X_{n-1}) \tag{2.8}$$

We can interpret this result as the building up of correlations between $X_1,\cdots,X_n$ and Y in n steps. In the first step, correlations between X_1 and Y are built up. Now, since X_1 is known (and therefore conditioned on), we proceed to build correlations between X_2 and Y. Now, X_1 and X_2 are known (and therefore conditioned on), so you proceed with building correlations between X_3 and Y. This goes on till all random variables have been exhausted. This same argument can be employed to build up correlations between $Y_1,\cdots,Y_n$ and X in

n steps, giving us the following result,

$$I(X;Y_1\cdots Y_n) = I(X;Y_1) + I(X;Y_2|Y_1) + \cdots + I(X;Y_n|Y_1,\cdots,Y_{n-1}) \tag{2.9}$$

This is easily justifiable via the symmetric property of mutual information.

As seen in Fig. 2.1, classical info-theoretic terms and their relation can be well understood from Venn diagrams. This is possible because all classical Shannon theoretic terms are positive quantities, conditioning can only reduce entropy, and mutual information is symmetric, non-negative, and it is defined as the amount by which 'uncertainty' is reduced for Bob about Alice's random variable X when he possesses Y. These arguments allow for the following equivalence [18]:

$$\begin{cases} H(X,Y) \leftrightarrow H(X \cup Y) \\ H(X;Y) \leftrightarrow H(X \cap Y) \\ H(X|Y) \leftrightarrow H(X \cap \neg Y) \\ H(Y|X) \leftrightarrow H(Y \cap \neg X) \end{cases} \tag{2.10}$$

It is precisely these equivalences that allow us to map classical Shannon terminologies to Venn diagrams.

2.2 Quantum Shannon Theory

Quantum Shannon theory is an extension of classical Shannon theory that quantifies the amount of information and correlations in quantum systems. The first fundamental measure is the von Neumann entropy. It is the quantum generalisation of the Shannon entropy that captures both classical and quantum uncertainty in a quantum state.

Suppose that Alice prepares some quantum system A in a state $\rho_A \in \mathcal{D}(\mathcal{H}_A)$ where $\mathcal{D}(\mathcal{H}_A)$ is the space of density operators defined on Hilbert space $\mathcal{H}_A$. Then, the entropy $S(\rho_A)$ associated with the state ρ_A is defined as

$$S(\rho_A) \equiv -\text{tr}\{\rho_A \log \rho_A\} \tag{2.11}$$

The density operator ρ_A, being Hermitian, has a spectral decomposition $\rho_A = \sum_x p_X(x) \left|x\right\rangle \left\langle x\right|$, then because ρ_A is diagonal in its eigenbasis, a relation between von Neumann entropy and

the Shannon entropy is obtained,

$$S(\rho_A) = -\mathrm{tr}\{\rho_A \log \rho_A\} = \sum_x p_X(x) \log p_X(x) = H(X) \tag{2.12}$$

Therefore, to calculate the von Neumann entropy of a density matrix ρ, all one would need to do is diagonalise ρ, obtain its eigenvalues $\{\lambda_k\}_k$ and calculate $\sum_k \lambda_k \log \lambda_k$. A useful property of von Neumann entropy is additivity, that is, for $\rho_A \in \mathcal{D}(\mathcal{H}_A)$ and $\sigma_B \in \mathcal{D}(\mathcal{H}_B)$, we have

$$S(\rho_A \otimes \sigma_B) = S(\rho_A) + S(\sigma_B) \tag{2.13}$$

There are other quantum entropic measures like joint von Neumann entropy, conditional von Neumann entropy and quantum mutual information, but for this thesis, it suffices to understand only the marginal von Neumann entropy $S(\rho_A)$ of a density operator ρ_A.

2.3 Quantum Measurements

2.3.1 Generalised Measurements

In quantum mechanics, a measurement is mathematically modelled by a set of measurement operators $\{M_k\}_k$ that satisfies the completeness relation,

$$\sum_k M_k^\dagger M_k = \mathcal{I} \tag{2.14}$$

where the probability for observing the outcome k when measuring a quantum state ρ is

$$p_K(k) = \mathrm{tr}(M_k \rho M_k^\dagger) \tag{2.15}$$

and the post-measurement state knowing that we measure outcome k is,

$$\frac{M_k \rho M_k^\dagger}{p_K(k)} \tag{2.16}$$

In a nutshell, the set of measurement operators $\{M_k\}_k$ provides enough information to define a unique post-measurement state and the probability of observing an outcome k.

2.3.2 POVM Formalism

Typically, in communication protocols, parties only care about the probability of obtaining a particular outcome, as that is how information is extracted from quantum systems. After this extraction, receivers do not care about the post-measurement state as it is usually discarded. In situations like these, a measurement is specified by a positive operator-valued measure (POVM). It is defined as follows:

A POVM is a set $\{\Lambda_k\}_k$ of Hermitian operators that satisfy non-negativity and completeness relation,

$$\forall k : \Lambda_k \geq 0, \qquad \sum_k \Lambda_k = \mathcal{I} \tag{2.17}$$

The probability of obtaining outcome k is

$$p_K(k) = \mathrm{tr}(\Lambda_k \rho) \tag{2.18}$$

The characterisation of a POVM measurement is more straightforward than earlier because POVM elements are Hermitian and positive semidefinite. It is clear that POVM is a type of generalised measurement where $\Lambda_k = M_k^\dagger M_k$. In this regard, going from a generalised measurement to a POVM allows us to specify a post-measurement state given in (2.16), but this is because we had the information of the measurement operators $\{M_k\}_k$, which allowed us to uniquely decompose $M_k = \sqrt{\Lambda_k}$. Without this information, from polar decomposition, we would have $M_k = U_k\sqrt{\Lambda_k}$, where U_k is an arbitrary unitary operator. This means a POVM measurement has no unique post-measurement state, which should not be problematic when post-measurement states are irrelevant.

2.3.3 Projective Measurements

Projection-valued measure (PVM) measurements, also referred to as von Neumann measurements, are the most natural type of measurement in quantum mechanics. A PVM is a complete set of orthogonal projectors $\{P_k\}_k$ satisfying the following three properties,

$$P_m P_n = \delta_{mn} P_m, \qquad P_k = P_k^\dagger, \qquad \sum_k P_k = \mathcal{I} \tag{2.19}$$

where the probability of obtaining an outcome associated with index k is

$$p_K(k) = \mathrm{tr}(P_k \rho) \tag{2.20}$$

and the post-measurement state after obtaining outcome k is

$$\frac{P_k \rho P_k}{p_K(k)} \tag{2.21}$$

In fact, it is through a PVM set that we construct an observable. Motivated by this, an alternate way to describe projective measurements through observables is as follows: A projective measurement is described by an observable, $\mathcal{A}$, a Hermitian operator on the state space of the system being observed. The observable, being Hermitian, has a spectral decomposition of the following form,

$$\mathcal{A} = \sum_n \lambda_n P_n \tag{2.22}$$

where P_n is the projector onto the eigenspace of $\mathcal{A}$ associated with eigenvalue λ_n. With this, the probability of measuring λ_n is $\mathrm{tr}(P_n\rho)$ where the quantum state after measurement is described using $\frac{P_n \rho P_n}{\mathrm{tr}(P_n \rho)}$. As it turns out, when physicists do experiments on quantum systems, the measurement performed is always a projective measurement. A POVM measurement is only implementable experimentally by performing a PVM measurement on a larger system described by a larger Hilbert space such that the effective measurement on the subsystem is a POVM measurement. This is mathematically modelled by Naimark's theorem, which shows that every POVM measurement is realisable as a PVM measurement on a larger Hilbert space.

2.4 Classical Information From Quantum Systems

2.4.1 Shannon Entropy of a POVM

Suppose Alice prepares a quantum state ρ and Bob performs a POVM $\{\Lambda_x\}$ on the system. The probability distribution $p_X(x)$ is defined by Born's rule as

$$p_X(x) = \mathrm{tr}(\Lambda_x \rho) \tag{2.23}$$

where X denotes the random variable corresponding to the classical output of the POVM.

Then, the Shannon entropy of the POVM measurement $\{\Lambda_x\}_x$ is defined as

$$H(X) = -\sum_x p_X(x) \log p_X(x) = -\sum_x \mathrm{tr}(\Lambda_x \rho) \log\{\mathrm{tr}(\Lambda_x \rho)\} \tag{2.24}$$

2.4.2 Accessible Information

Suppose Alice prepares an ensemble $\mathcal{E} = \{p_X(x), \rho_x\}$ and Bob wants to retrieve as much information as possible about the random variable X from the ensemble $\mathcal{E}$. To do so, Bob performs a POVM measurement $\{\Lambda_y\}_y$ and obtains information on the classical outputs of the POVM. Let these classical outputs be realisations of a random variable Y. Then, the mutual information $I(X;Y)$ is the information Bob has about X, given he possesses the Y. Because Bob wants to retrieve as much information as possible about X, and he has the freedom to choose his measurements, he will need to perform a measurement that maximises his information about X. The resultant mutual information he obtains is referred to as the 'Accessible Information' $I_{acc}(\mathcal{E})$ of the ensemble $\mathcal{E}$ and is given by

$$I_{acc}(\mathcal{E}) \equiv \max_{\{\Lambda_y\}_y} I(X;Y) = \max_{\{\Lambda_y\}_y} \{H(Y) - H(Y|X)\} \tag{2.25}$$

where $H(Y)$ is the Shannon entropy of the POVM $\{\Lambda_y\}_y$, $H(Y|X)$ is defined by $p_X(y|x) = \mathrm{tr}(\Lambda_y \rho_x)$ and $p_{X,Y}(x,y) = p_X(x)p_X(y|x)$.

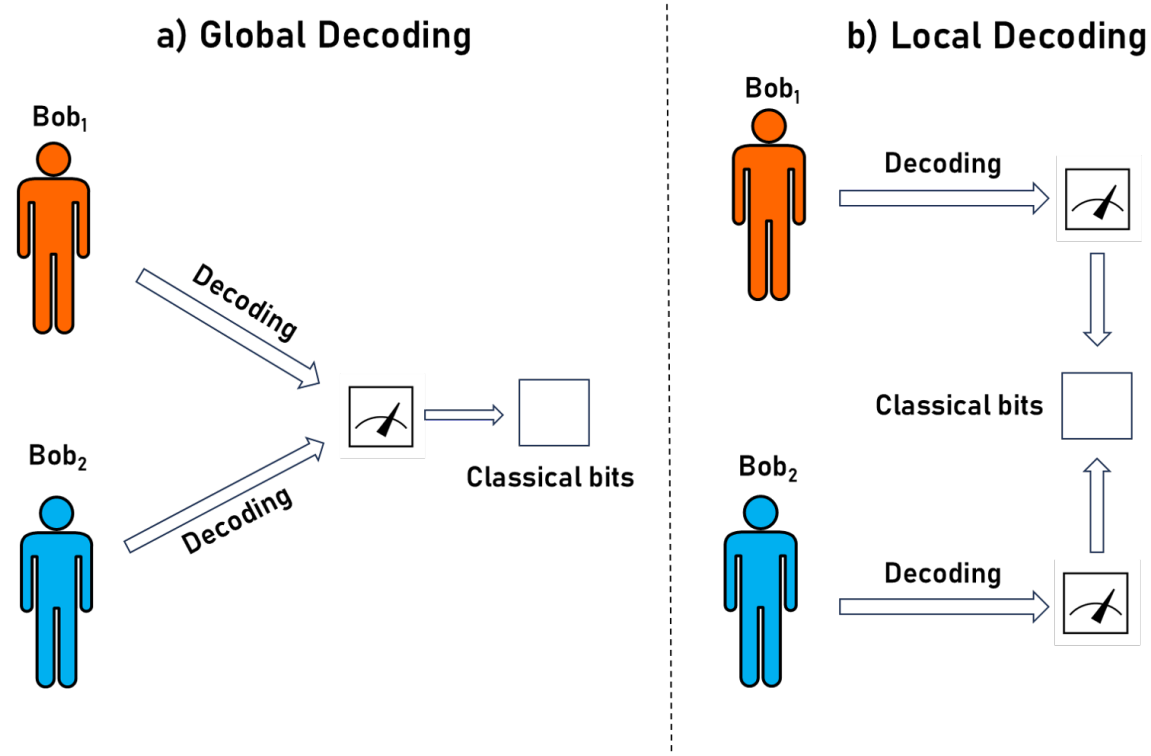

Figure 2.2: In **a)**, receivers Bob_1 and Bob_2 employ a global measurement strategy where they perform a joint measurement. In **b)**, receivers individually perform local measurements on the ensemble they possess to extract information.

The maximisation in the definition of I_{acc} is generally hard to compute, so we rely on useful upper bounds. The most important bound is the Holevo bound and is given by

$$I_{acc}(\mathcal{E}) \leq \chi(\mathcal{E}) = S(\rho_{\mathcal{E}}) - \sum_{x \in \mathcal{X}} p_X(x) S(\rho_{AB}^x) \tag{2.26}$$

where $\chi(\mathcal{E})$ is referred to as the Holevo quantity or Holevo *chi* of the ensemble $\mathcal{E}$. The Holevo bound is saturable in the asymptotic limit in the sense there exists a particular encoding and decoding scheme that asymptotically attains the bound if the sender could send long strings of the input quantum states ρ_x.

The Holevo bound tells a crucial fact: The maximum classical information that can be decodable by sending a d-dimensional quantum system is $\log d$ bits. This means the maximum amount of information that can be sent via n qubits through a noiseless quantum channel is bounded by n bits. In this sense, classical communication with quantum systems does not give any advantage.

2.4.3 Locally Accessible Information

Consider two parties, Alice and Bob, together sharing an ensemble $\mathcal{E} = \{p_X(x), \rho_{AB}^x\}$ given to them by a third party, and they want to retrieve information about random variable X. The restriction here is that Alice and Bob are far away and can only employ Local Operations and Classical Communication (LOCC) type measurements.

A LOCC protocol (see Fig. 2.3) can be described like this: Alice and Bob share a state $\rho_{AB} \in \mathcal{D}(\mathcal{H}_A \otimes \mathcal{H}_B)$ where $\mathcal{D}(\mathcal{H})$ is the set of density operators defined on a Hilbert space $\mathcal{H}$. Without loss of generality, Alice starts a LOCC protocol by performing a quantum operation $\{\mathcal{A}_x^{(1)}\}_x$, satisfying $\sum_x (\mathcal{A}_x^{(1)})^\dagger \mathcal{A}_x^{(1)} = \mathcal{I}_A$ on her part of the system defined by the local Hilbert space $\mathcal{H}_A$, and sends her measurement result x to Bob via a classical channel. Depending on what Alice sent, Bob will perform a quantum operation $\{\mathcal{B}_{xy}^{(1)}\}_y$, satisfying $\sum_y (\mathcal{B}_{xy}^{(1)})^\dagger \mathcal{B}_{xy}^{(1)} = \mathcal{I}_B$ on his part of the system defined by the local Hilbert space $\mathcal{H}_B$. If the LOCC protocol stops here, then it is referred to as a one-way LOCC protocol. This is because classical information is only one-way here, i.e. from Alice (who begins the protocol) to Bob. Now, Bob can send his result y back to Alice via a classical channel, and depending on what Alice receives from Bob, she performs a quantum operation $\{\mathcal{A}_{xyz}^{(2)}\}_z$, satisfying $\sum_z (\mathcal{A}_{xyz}^{(2)})^\dagger \mathcal{A}_{xyz}^{(2)} = \mathcal{I}_A$. Alice can end the protocol here or continue by sending her measurement outcome z to Bob via a classical channel. This can go on indefinitely for

infinite rounds. For any given number of rounds, the overall protocol can be referred to as a two-way LOCC protocol. It is to be noted that the above description is a LOCC protocol between two parties. LOCC protocols can be non-trivially generalised to multiple parties, and its detailed description is given in [14].

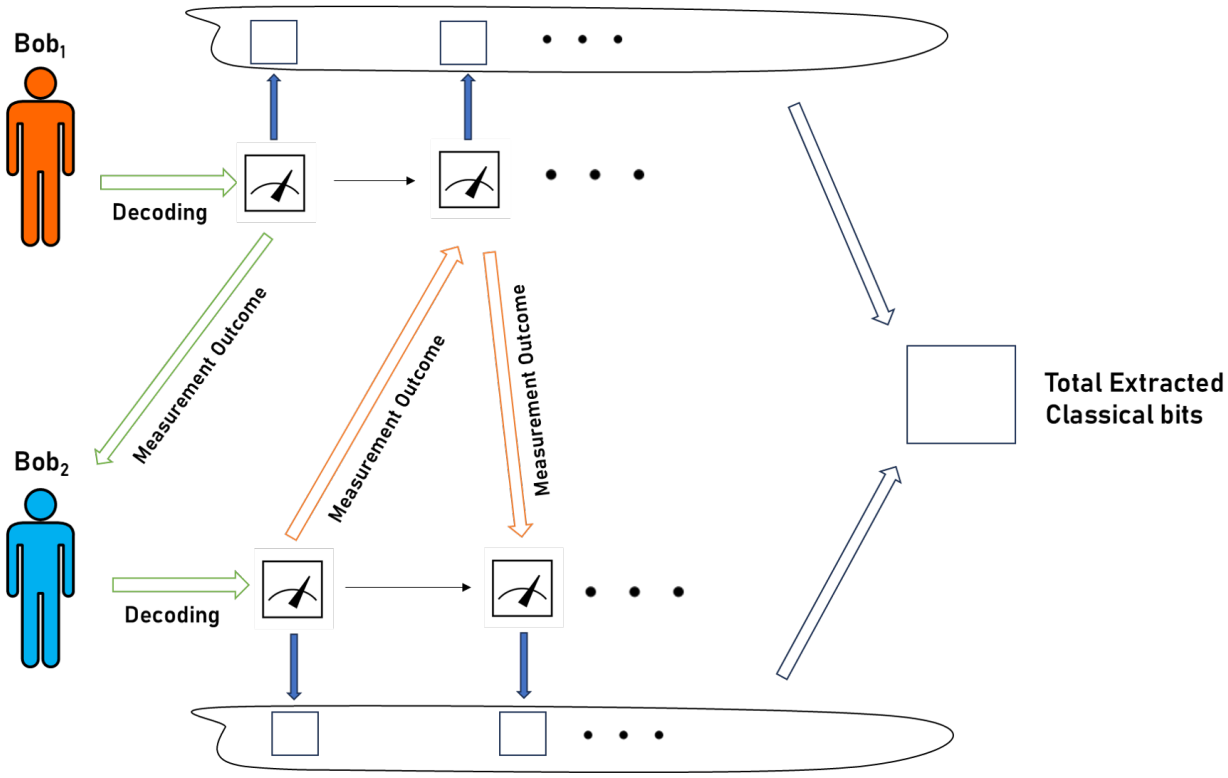

Figure 2.3: Two receivers employ a LOCC decoding scheme where Bob_1 begins the protocol. If the protocol stops with one-way communication employed (shown in green), then it is referred to as a one-way LOCC ($\texttt{LOCC}_1$) decoding scheme. If the classical communication is through both ways (both green and orange), then it is referred to as a two-way LOCC ($\texttt{LOCC}_2$) decoding scheme.

In such scenarios, we can define a quantity referred to as 'locally accessible information' of an ensemble I_{acc}^{LOCC}, given by

$$I_{acc}^{LOCC} = \max_{\mathcal{P}} I(X;Y) \tag{2.27}$$

where $\mathcal{P}$ is the class of all LOCC measurement protocols.

Like globally accessible information, there are no methods to calculate locally accessible information analytically, and it is even more complex because the set of LOCC measurements has no tractable characterisation [14]. Nevertheless, an upper bound to locally accessible

information was provided in [3], taking the form:

$$I_{acc}^{LOCC} \leq S(\rho_A) + S(\rho_B) - \max_{Z=A,B} \sum_{x \in \mathcal{X}} p_X(x) S(\rho_Z^x) \tag{2.28}$$

where $\mathcal{E} = \{p_X(x), \rho_{AB}^x\}$ is the bipartite ensemble possesses by Alice and Bob, ρ_A and ρ_B are reductions of $\rho_{\mathcal{E}} = \sum_x p_X(x)\rho_{AB}^x$, and ρ_Z^x is a reduction of ρ_{AB}^x. Unfortunately, unlike the Holevo bound, this Holevo-like bound cannot be universally saturated for all ensembles, even in the asymptotic limit. However, some examples of ensembles do saturate it in $\mathbb{C}^n \otimes \mathbb{C}^n$ systems [3].

A slightly stronger bound has been found in [29], a generalisation of the Holevo-like bound, given by

$$\begin{aligned} I_{acc}^{LOCC} &\leq S(\rho_A) + S(\rho_B) - \sum_{x \in \mathcal{X}} p_X(x) S(\rho_B^x) \\ &- \sum_{n_1, n_2, \cdots, (n_m)} p_{N_1, N_2, \cdots (N_M)}(n_1, n_2, \cdots, (n_m)) S\left(\sum_x p_{X|N_1, N_2, \cdots (N_M)}(x|n_1, n_2, \cdots, (n_m)) \rho_A^{x|n_1 n_2 \cdots n_m} \right) \end{aligned} \tag{2.29}$$

where $\{p_{X|N_1,N_2,\cdots(N_M)}(x|n_1, n_2, \cdots, (n_m)), \rho_{AB}^{x|n_1 n_2 \cdots n_m}\}$ is the post-measurement ensemble obtained after the measurement in the ${n_m}^{th}$ step, and $p_{X|N_1,N_2,\cdots(N_M)}(x|n_1, n_2, \cdots, (n_m))$ is the probability of the sequence of measurement outcomes in steps $1, 2, \cdots, n$. Even this bound is not asymptotically saturable, and unlike the previous bound, this is particularly hard to calculate.

Chapter 3

Quantum Dense Coding

Quantum dense coding protocol, also called super-dense coding, is a classical communication protocol that uses quantum systems as information carriers and leverages non-local resources like entanglement to transmit more classical information than would be possible in any classical communication protocol. By leveraging pre-shared entanglement, one can "bypass" the Holevo bound and decode more than a bit of classical information by sending only a single qubit. We will describe a dense coding protocol for a single sender and single receiver and extend it to the distributed scenario with multiple senders and up to two receivers.

3.1 Single Sender and Single Receiver

Consider a single sender, Alice (A), and a single receiver, Bob (B), sharing a quantum state $\rho_{AB} \in \mathbb{C}^{d_A} \otimes \mathbb{C}^{d_B}$, where $\mathbb{C}^{d_{A(B)}}$ denotes the complex Hilbert space of the subsystem, $A(B)$. Let X be a random variable whose realisations x are *letters* in an *alphabet* $\mathcal{X}$. A general dense coding protocol between a single sender and a single receiver (see Fig. 3.1) can be described in three steps [7]:

1. **Encoding**: Alice encodes information in the form of a random variable X on her part of ρ_{AB}. The encoding process involves the application of a local unitary operator, U_A^x, with probability $p_X(x)$ on Alice's subsystem. As a result, the state ρ_{AB} gets converted to an encoded ensemble $\mathcal{E} = \{p_X(x), \rho_{AB}^x\}$, where $\rho_{AB}^x = (U_A^x \otimes \mathcal{I}_{d_B})\rho_{AB}(U_A^{x\dagger} \otimes \mathcal{I}_{d_B})$ and $x \in \mathcal{X}$ are realisations of the random variable X.

2. **Sending**: Alice deterministically sends *her part* of the ensemble state to Bob through

a quantum channel. For our purpose, we will consider it to be a noiseless quantum channel.

3. **Decoding**: Since Alice sends her part of the ensemble to Bob, the whole ensemble $\mathcal{E} = \{p_X(x), \rho^x_{AB}\}$, is now with Bob. Bob tries to extract maximal information about the random variable X from the ensemble by performing suitable measurements $\{\Lambda^B_y\}_y$ where y are realisations of the random variable Y such that the mutual information $I(X;Y)$ is maximised.

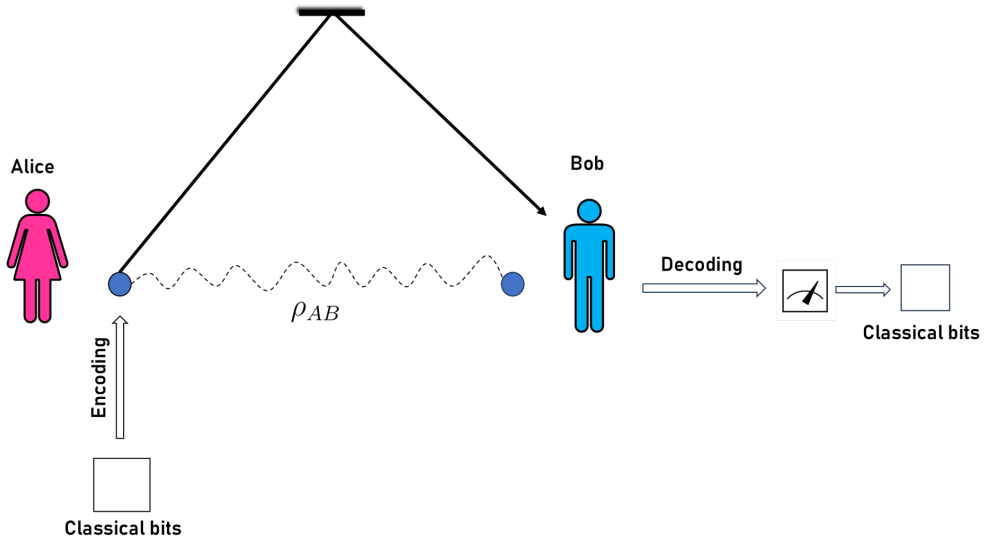

Figure 3.1: A standard dense coding protocol with a single sender, Alice, and a single receiver, Bob, sharing a state ρ_{AB}. It involves encoding classical information onto Alice's subsystem, sending her system to Bob and decoding encoded information via suitable measurements.

The accessible information, I_{acc} of the encoded ensemble $\mathcal{E}$ is upper bounded by the Holevo quantity $\chi(\mathcal{E}) = S(\rho_\mathcal{E}) - \sum_{x\in\mathcal{X}} p_X(x) S(\rho^x_{AB})$ where $\rho_\mathcal{E} = \sum_x p_X(x)\rho^x_{AB}$ is the density matrix representing the encoded ensemble. Then, we define the dense coding capacity of a dense-coding protocol to be

$$\begin{aligned} \chi_{DC} &= \max_{|\mathcal{X}|} \max_{U^x_A, p_X(x)} \chi(\mathcal{E}) \\ &= \max_{|\mathcal{X}|} \max_{U^x_A, p_X(x)} \left(S(\rho_\mathcal{E}) - \sum_{x\in\mathcal{X}} p_X(x) S(\rho_x) \right), \end{aligned} \tag{3.1}$$

It was shown that in [7] that for the protocol described above, after performing the necessary

optimisations, χ_{DC} is given by

$$\chi_{DC} = \log(d_A) + S(\rho_B) - S(\rho_{AB}) \tag{3.2}$$

where the form of allowed encodings taking the form $\{p_X(x), U_A^x\}$ that maximise the Holevo quantity looks like $\{\frac{1}{d_A^2}, M_k\}$ where the set $\{M_k\}_{k=0}^{d_A^2-1}$ is a complete set of mutually orthogonal unitary operators that obey the trace rule $\frac{1}{d_A^2}\sum_k M_j^\dagger Q M_k = \mathrm{tr}(Q)$ for any operator Q. An example that satisfies these conditions is given by the group of shift-and-multiply operators [27],

$$M_{(p,q)}\,|j\rangle = \exp\left\{i\frac{2\pi}{d}pj\right\}|j+q(\mathrm{mod}\ d_A)\rangle$$

where $k \equiv (p,q)$ and $p,q,j \in \{0,1,\cdots,d_A-1\}$. An intuitive reason why these unitaries are optimal for encoding is that the set of shift-and-multiply operators forms a complete set of mutually orthogonal unitary operators. Therefore, their application on state ρ would 'mix' it the most, making each realisation of the encoded ensemble ρ_{AB}^x as distinguishable as possible, thereby allowing for a larger entropy associated with the density matrix representing the encoded ensemble. Interestingly, for qubits ($d_A = 2$), the group of shift-and-multiply operators is $\{\mathcal{I}, \sigma_x, \sigma_z, \sigma_x\sigma_z\}$.

It is clear from (3.2) that any state ρ_{AB} satisfying $S(\rho_B) > S(\rho_{AB})$ gives an advantage over classical communication protocols; we say that these states are "dense-codable". As it turns out, bound entangled states are precisely those that do not satisfy this condition and are, therefore, not useful in dense-coding protocols [7].

Since the Holevo bound can be asymptotically saturated, the DC capacity, in some sense, tells us the maximum amount of classical information that a sender can transmit to a receiver given they start with a particular shared quantum state ρ_{AB}. Clearly, χ_{DC} is maximum for a pure state $\rho_{AB} = |\psi\rangle\langle\psi|$ where $|\psi\rangle$ is maximally entangled where $\chi_{DC}^{max} = \log d_A d_B$. Although we are just sending a d_A-dimensional state, the Holevo bound is still valid as long as we consider the pre-shared entanglement, as then the dimension of the quantum system under consideration is $d_A d_B$ and not d_A.

3.2 Multiple Senders and Single Receiver

Consider $N-1$ Alices $(A_1, A_2, \cdots, A_{N-1})$ and a single Bob (B), all sharing an N-party quantum state $\rho = \rho_{A_1,\cdots,A_{N-1},B}$. The j^{th} Alice A_j applies unitary $U_{A_j}^{x_j}$ with probability $p_{A_j}^{x_j}$

to her part of the state ρ. All Alices do the encoding and send their state to Bob. The whole ensemble $\{r_X(x), \vartheta_x\}$ is now with Bob, where

$$r_X(x) = \prod_{j=1}^{N-1} p_{A_j}^{x_j}, \quad \vartheta_x = \left(\bigotimes_{j=1}^{N-1} U_{A_j}^{x_j} \otimes \mathcal{I}_{d_B}\right) \rho \left(\bigotimes_{j=1}^{N-1} U_{A_j}^{x_j\,\dagger} \otimes \mathcal{I}_{d_B}\right) \tag{3.3}$$

Since Bob possesses the whole ensemble, he can perform optimal measurements to extract information. The DC capacity in this scenario is

$$\chi^{A_1,A_2,\cdots,A_{N-1},B} = \left[\sum_{j=1}^{N-1} \log(d_{A_j})\right] + S(\rho_B) - S(\rho_{A_1,\cdots,A_{N-1},B}) \tag{3.4}$$

This is the same as (3.2) where $A \equiv A_1 A_2 \cdots A_{N-1}$.

3.3 Multiple Senders and Two Receivers

Consider $N-1$ Alices $(A_1, A_2, \cdots, A_{N-1})$ and two Bobs (B_1 and B_2), all sharing an $(N+1)$-party quantum state $\rho = \rho_{A_1,\cdots,A_{N-1},B_1,B_2}$. The j^{th} Alice A_j applies a unitary $U_{A_j}^{x_j}$ with probability $p_{A_j}^{x_j}$ to her part of the state ρ. Now, the first k Alices $A_1, \cdots A_k$ send their quantum systems to B_1 and the remaining Alices $A_{k+1}, \cdots, A_{N-1}$ send their part of states to B_2. Now, both Bobs together possess the whole ensemble $\mathcal{E} = \{r_X(x), \vartheta_x\}$ where

$$r_X(x) = \prod_{j=1}^{N-1} p_{A_j}^{x_j}, \quad \vartheta_x = \left(\bigotimes_{j=1}^{N-1} U_{A_j}^{x_j} \otimes \mathcal{I}_{d_{B_1}} \otimes \mathcal{I}_{d_{B_2}}\right) \rho \left(\bigotimes_{j=1}^{N-1} U_{A_j}^{x_j\,\dagger} \otimes \mathcal{I}_{d_{B_1}} \otimes \mathcal{I}_{d_{B_2}}\right) \tag{3.5}$$

Unlike the previous case, we now have two receivers who will extract information from the ensemble $\mathcal{E}$. Depending on how far these two receivers are, we will have three possible decoding scenarios: (1) Global Decoding, (2) Local Decoding and (3) LOCC Decoding.

3.3.1 Global Decoding

If both the Bobs are close enough, they can afford to perform global measurements. In this scenario, they can be effectively treated as a single receiver $B \equiv B_1 B_2$. Then, the DC capacity in this scenario is the same as others

$$\chi^{A_1,\cdots,A_{N-1},B_1,B_2} = \left[\sum_{j=1}^{N-1} \log(d_{A_j})\right] + S(\rho_{B_1,B_2}) - S(\rho_{A_1,\cdots,A_{N-1},B_1,B_2}) \tag{3.6}$$

The crux here is that by effectively treating both the Bobs to be a single receiver, this scenario simplifies to a single receiver case, and its treatment is already discussed in section 3.2. The DC capacity in this scenario is called the global DC (G-DC) capacity.

3.3.2 Local Decoding

If both Bobs are far away and do not have access to a stable classical communication channel, then the best they can do is perform local measurements on the parts they have received. Noting that the first k Alices send their encoded quantum systems to B_1 and the remaining Alices send it to B_2, this situation can be effectively treated as two separate dense coding protocols, each being equivalent to the situation discussed in section 3.2. Therefore, the DC capacity simplifies to:

$$\chi^{A_1,\cdots,A_{N-1},B_1,B_2} = \chi^{A_1,\cdots,A_k,B_1} + \chi^{A_{k+1},\cdots,A_{N-1},B_2} \tag{3.7}$$

The above result tells us that the overall dense coding capacities, $\chi^{A_1,\cdots,A_{N-1},B_1,B_2}$, is the sum of the dense coding capacities of two independent dense coding protocols, each given by $\chi^{A_1,\cdots,A_k,B_1}$ and $\chi^{A_{k+1},\cdots,A_{N-1},B_2}$, respectively.

3.3.3 LOCC Decoding

If both Bobs are far away but have access to a stable classical communication channel, then the best they can do is perform a larger class of operations known as LOCC. The receivers B_1 and B_2 are allowed to apply LOCC strategies in the bipartite cut $A_1\cdots A_kB_1 : A_{k+1}\cdots A_{N-1}B_2$. Since the set of LOCC operations has no tractable characterisation, we will have to resort to the Holevo-like bound we discussed in section 2.4.3. If χ^{LOCC} is the LOCC-DC capacity, then it will be upper bounded by the maximisation of the Holevo-like bound over all possible encoding strategies,

$$\chi^{LOCC} \leq \max\left\{ S(\bar{\vartheta}^{(1)}) + S(\bar{\vartheta}^{(2)}) - \max_{i=1,2} \sum_x r_X(x) S(\vartheta_x^{(i)}) \right\} \tag{3.8}$$

where $\bar{\vartheta} = \sum_x r_X(x)\vartheta_x$, $\vartheta_x^{(1)} = \mathrm{tr}_{A_{k+1}\cdots A_{N-1}B_2}(\vartheta_x)$, $\vartheta_x^{(2)} = \mathrm{tr}_{A_1\cdots A_kB_1}(\vartheta_x)$, $\bar{\vartheta}^{(1)} = \mathrm{tr}_{A_{k+1}\cdots A_{N-1}B_2}(\bar{\vartheta})$ and $\bar{\vartheta}^{(2)} = \mathrm{tr}_{A_1\cdots A_kB_2}(\bar{\vartheta})$ where the maximisation is over all possible choices of unitaries and probabilities by the Alices. This maximisation has been performed in [7], and an upper-

bound to the LOCC-DC capacity is given by,

$$\chi^{LOCC} \leq \left[\sum_{j=1}^{N-1} \log(d_{A_j})\right] + S(\rho_{B_1}) + S(\rho_{B_2}) - \max_{x=1,2} S(\rho_x) \equiv \mathcal{B}^{LOCC} \tag{3.9}$$

where $\rho_1 = \mathrm{tr}_{A_{k+1}\cdots A_{N-1}B_2}(\rho)$, $\rho_2 = \mathrm{tr}_{A_1\cdots A_k B_1}(\rho)$, $\rho_{B_1} = \mathrm{tr}_{A_1\cdots A_{N-1}B_2}(\rho)$ and $\rho_{B_2} = \mathrm{tr}_{A_1\cdots A_{N-1}B_1}(\rho)$.

Unlike G-DC capacity, which is asymptotically reachable, $\mathcal{B}^{LOCC}$ is not always asymptotically reachable because the Holevo-like bound is not asymptotically saturable. Nevertheless, this is the only known upper bound to χ^{LOCC}.

3.4 Dense Coding With GHZ State

To compare the standard dense coding protocol with a similar scenario that we will soon consider in the following chapter, it is convenient to inspect the standard dense coding protocol involving a single sender, Alice, and two receivers, Bob_1 and Bob_2. For a global decoding scenario, the two-receiver case can effectively be considered as a single receiver $B \equiv B_1B_2$ (see Fig. 3.2).

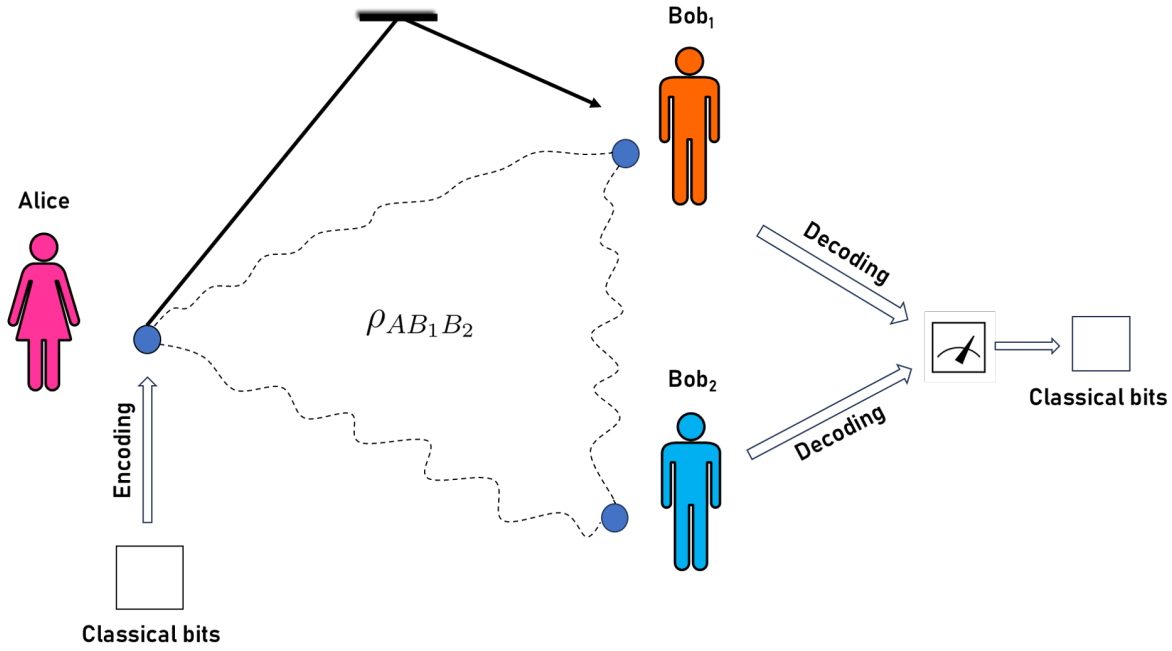

Figure 3.2: A standard dense coding protocol with a single sender and two receivers sharing a state $\rho_{AB_1B_2} = |gGHZ\rangle$ where global decoding strategies are considered.

Let us suppose that in the two-receiver scenario, Alice, Bob_1 and Bob_2 share a generalised GHZ state $|gGHZ\rangle_{AB_1B_2} = \cos(\theta/2)\,|000\rangle + e^{i\phi}\sin(\theta/2)\,|111\rangle$, where $\theta \in [0,\pi]$ and $\psi \in [0,2\pi]$. Here, $d_A = 2$, and so the optimal unitary operators used for encoding are given by $S = \{\mathcal{I}, \sigma_z, \sigma_x, \sigma_x\sigma_z\}$, each of which is applied with equal probability. Following this, Alice deterministically sends her part of the qubit to party B. Because the shared state is a pure state, the Holevo bound reduces to just the von Neumann entropy of the encoded ensemble. The DC capacity in this scenario would be to calculate the von Neumann entropy of the optimal encoded ensemble. Normally, the density matrix associated with the encoded ensemble is

$$\rho_{\mathcal{E}} = \sum_i p_i \left[\cos\left(\frac{\theta}{2}\right) U_i^A\,|000\rangle + e^{i\phi}\sin\left(\frac{\theta}{2}\right) U_i^A\,|111\rangle \right] \left[\cos\left(\frac{\theta}{2}\right) \langle 000|\, U_i^{A\dagger} + e^{-i\phi}\sin\left(\frac{\theta}{2}\right) \langle 111|\, U_i^{A\dagger} \right] \tag{3.10}$$

This is simplified to

$$\rho^{\mathcal{E}} = \sum_i p_i \left[\cos^2\left(\frac{\theta}{2}\right) U_i^A\,|000\rangle\langle 000|\, U_i^{A\dagger} + \sin^2\left(\frac{\theta}{2}\right) U_i^A\,|111\rangle\langle 111|\, U_i^{A\dagger} + e^{i\phi}\sin\left(\frac{\theta}{2}\right)\cos\left(\frac{\theta}{2}\right) U_i^A\,|111\rangle\langle 000|\, U_i^{A\dagger} + e^{-i\phi}\sin\left(\frac{\theta}{2}\right)\cos\left(\frac{\theta}{2}\right) U_i^A\,|000\rangle\langle 111|\, U_i^{A\dagger} \right] \tag{3.11}$$

Setting $p_i = \frac{1}{4}\ \forall\ i$ and picking $U_i^A \in S$, the optimal encoded ensemble is

$$\rho^{\mathcal{E}} = \frac{1}{2}\left[\cos^2\left(\frac{\theta}{2}\right)\left(|000\rangle\langle 000| + |100\rangle\langle 100| \right) + \sin^2\left(\frac{\theta}{2}\right)\left(|111\rangle\langle 111| + |011\rangle\langle 011| \right) \right] \tag{3.12}$$

The matrix inside is already in diagonal form; the non-zero eigenvalues are: $\frac{1}{2}\cos^2\left(\frac{\theta}{2}\right)$, $\frac{1}{2}\cos^2\left(\frac{\theta}{2}\right)$, $\frac{1}{2}\sin^2\left(\frac{\theta}{2}\right)$ and $\frac{1}{2}\sin^2\left(\frac{\theta}{2}\right)$. This gives the von Neumann entropy, which is the DC capacity in our case, to be

$$\chi_{SDC} = S(\rho^{\mathcal{E}}) = 1 - 2\left\{ \cos^2\left(\frac{\theta}{2}\right)\log\left[\cos\left(\frac{\theta}{2}\right)\right] + \sin^2\left(\frac{\theta}{2}\right)\log\left[\sin\left(\frac{\theta}{2}\right)\right] \right\} \tag{3.13}$$

where SDC refers to Standard Dense Coding. The above result holds even when we consider the situation with a single sender, Alice, and multiple receivers, $\text{Bob}_1 \cdots \text{Bob}_{M-1}$, sharing a M-dimensional GHZ state because we can treat $B \equiv B_1 \cdots B_{M-1}$.

As expected, the DC capacity is independent of the phase, reaches the maximum at $\chi_{max} = 2$ at $\theta = \frac{\pi}{2}$ when generalised GHZ is maximally entangled and is symmetric about $\theta = \frac{\pi}{2}$. Unless Alice possesses two qubits of the GHZ state, there is no way Alice can reach all eight 3-qubit GHZ states through local unitary transformations and go past 2 bits of DC capacity [10].

Chapter 4

Dense Coding With Non-Classical Routing

Before we get into the idea of non-classical routing in a dense coding protocol, it will be useful to introduce the method of multiplexing unitaries with the aid of a coherent quantum system. This will help us in formulating a compact, mathematical description of our protocol. The following discussion is based on our work in [31].

4.1 Unitary Multiplexing

Consider two given unitary operators, U and V, a target system ρ_t and a control system ρ_c. A controlled unitary operator of the form, $W = U \otimes |0\rangle\langle 0|_c + V \otimes |1\rangle\langle 1|_c$, acts on the composite state of the system and control [1]. If we set the control to be $\rho_c = |+\rangle\langle +|$, then the joint state of the system and control obtained after the unitary evolution is

$$\mathcal{N}(U,V)(\rho_t \otimes \rho_c) = W(\rho_t \otimes \rho_c)W^\dagger = \frac{1}{2}\Big(U\rho_t U^\dagger \otimes |0\rangle\langle 0| + U\rho_t V^\dagger \otimes |0\rangle\langle 1| + V\rho_t U^\dagger \otimes |1\rangle\langle 0| + V\rho_t V^\dagger \otimes |1\rangle\langle 1| \Big) \quad (4.1)$$

If we consider a pure state input, i.e. $\rho_t = |\psi\rangle\langle\psi|$, we observe that the above equation simplifies to

$$\mathcal{N}(U,V)(\rho_t \otimes \rho_c) = |\Psi\rangle\langle\Psi| \quad (4.2)$$

where $|\Psi\rangle = \frac{1}{\sqrt{2}}\big[(U|\psi\rangle) \otimes |0\rangle + (V|\psi\rangle) \otimes |1\rangle\big]$. Now, a measurement is performed on the control system in the Hadamard basis, $\{|+\rangle\langle+|, |-\rangle\langle-|\}$, and the outcome corresponding to $|+\rangle\langle+|$ is post-selected. This causes the target system to collapse into the unnormalised state $|\phi\rangle$, given by

$$|\phi\rangle = \frac{1}{2}(U+V)|\psi\rangle . \tag{4.3}$$

Using this strategy, we can thus multiplex unitaries U and V using a control quantum system. We will employ such multiplexing to model our dense coding protocol.

4.2 Protocol

Consider a single sender, Alice (A), and two receivers, Bob_1 (B_1) and Bob_2 (B_2). They share a tripartite pure state $|\psi\rangle_{AB_1B_2}$. Let Bob_1 and Bob_2 have access to auxiliary systems $|0\rangle_{C_{B_1}}$ and $|0\rangle_{C_{B_2}}$, which they can use whenever required. The two receivers, Bob_1 and Bob_2, reside in laboratories L_1 and L_2, respectively. Depending on to whom Alice wants to send her quantum system, the following two situations can arise:

- **Process 1**: Alice applies local unitaries U^x with probability $p_X(x)$ to her part of the tripartite state and sends her quantum system to lab L_1 via a noiseless quantum channel. Once sent, we formally define the labs as *ordered* quantum systems $L_1 \equiv (B_1, A)$ and $L_2 \equiv (B_2, C_{B_2})$. The ensemble possessed by the two receivers together is

$$\left\{p_X(x), U_2^x|\psi\rangle_{L_1L_2}\right\} \equiv \left\{p_X(x), (\mathcal{I}_{B_1} \otimes U^x \otimes \mathcal{I}_{B_2} \otimes \mathcal{I}_{C_{B_2}})|\psi\rangle_{B_1A:B_2C_{B_2}}\right\} \tag{4.4}$$

  This configuration is associated with the control state $\rho_c = |0\rangle\langle 0|$.

- **Process 2**: Alice applies local unitaries V^x with probability $p_X(x)$ to her share of the tripartite state and sends her quantum system to lab L_2 via a noiseless quantum channel. Once sent, like earlier, we define the two labs as *ordered* quantum systems $L_1 \equiv (B_1, C_{B_1})$ and $L_2 \equiv (B_2, A)$. The ensemble with the two receivers together, in this case, is

$$\left\{p_X(x), V_4^x|\psi\rangle_{L_1L_2}\right\} \equiv \left\{p_X(x), (\mathcal{I}_{B_1} \otimes \mathcal{I}_{C_{B_1}} \otimes \mathcal{I}_{B_2} \otimes V^x)|\psi\rangle_{B_1C_{B_1}:B_2A}\right\} \tag{4.5}$$

  This configuration is associated with the control state $\rho_c = |1\rangle\langle 1|$.

We aim to create a superposition of these two processes by setting the control state to be

$\rho_c = |+\rangle\langle+|$, in which case the sending itself becomes neither deterministic nor probabilistic but completely non-classical. Our idea is to employ another quantum system, referred to as the "control", which coherently controls the above two processes. We will proceed with the assumption that the superposition of the above two processes is possible. Similar to the formalism provided after (4.2), a measurement is performed on the control qubit in the Hadamard basis. Now, if the state collapses to $|+\rangle$ after the measurement, then the state possessed at the receivers' end is given by

$$|\Psi_x\rangle = \frac{1}{\sqrt{\langle\Psi_x|\Psi_x\rangle}} \left(U_2^x |\psi\rangle_{L_1L_2} + V_4^x |\psi\rangle_{L_1L_2}\right). \tag{4.6}$$

The state $|\psi\rangle_{L_1L_2}$ next to V_4^x is the same as the one next to U_2^x but with the 2nd and 4th indices swapped. Therefore

$$|\Psi_x\rangle = \frac{1}{\sqrt{\langle\Psi_x|\Psi_x\rangle}} \left(U_2^x + V_4^x \cdot \texttt{SWAP}_{2,4}\right) |\psi\rangle_{L_1L_2} \tag{4.7}$$

where $\texttt{SWAP}_{2,4}$ is a SWAP unitary acting on indices 2 and 4 occurring due to the routing of Alice's state. By indices, we mean the order of the qubit, with index 1 being the left-most qubit. Here, the SWAP unitary arises naturally due to Alice choosing to route her system to either lab L_1 or L_2. The purpose of including auxiliary systems is to ensure that the dimensions of L_1 and L_2 are consistent in each term of the superposition.

In the dense coding protocol that we consider, Alice encodes a pair of unitaries, $\{U^x, V^x\}$, via multiplexing and "non-classically" routes them to laboratories L_1 and L_2, respectively. Note that the multiplexing is not independent of the routing but is the very thing that leads to non-classical routing. This results in the state shared between L_1 and L_2 to be $|\Psi_x\rangle$, as seen in (4.6). If $|\Psi_x\rangle$ is created with probability $p_X(x)$, then the encoded ensemble possessed by laboratories L_1 and L_2 is given by $\mathcal{E} \equiv \{p_X(x), \rho_x = |\Psi_x\rangle\langle\Psi_x|\}$. Looking at (4.7), it can be seen that the whole superposition of 'processes' can be modelled by an effective unitary operation W_x on the joint state of the system and control, followed by performing a measurement on the control system in the Hadamard basis and post-selecting those states for which the control collapses to $|+\rangle$. The effective unitary operation is given by $\mathcal{N}(U_2^x, V_4^x)(\rho \otimes \rho_c) = W_x(\rho \otimes \rho_c)W_x^\dagger$, where the global unitary is of the form

$$W_x = (\mathcal{I}_{B_1} \otimes U^x \otimes \mathcal{I}_{B_2} \otimes \mathcal{I}_{C_{B_2}}) \otimes |0\rangle\langle 0| + (\mathcal{I}_{B_1} \otimes \mathcal{I}_{C_{B_1}} \otimes \mathcal{I}_{B_2} \otimes V^x) \cdot \texttt{SWAP}_{2,4} \otimes |1\rangle\langle 1|. \tag{4.8}$$

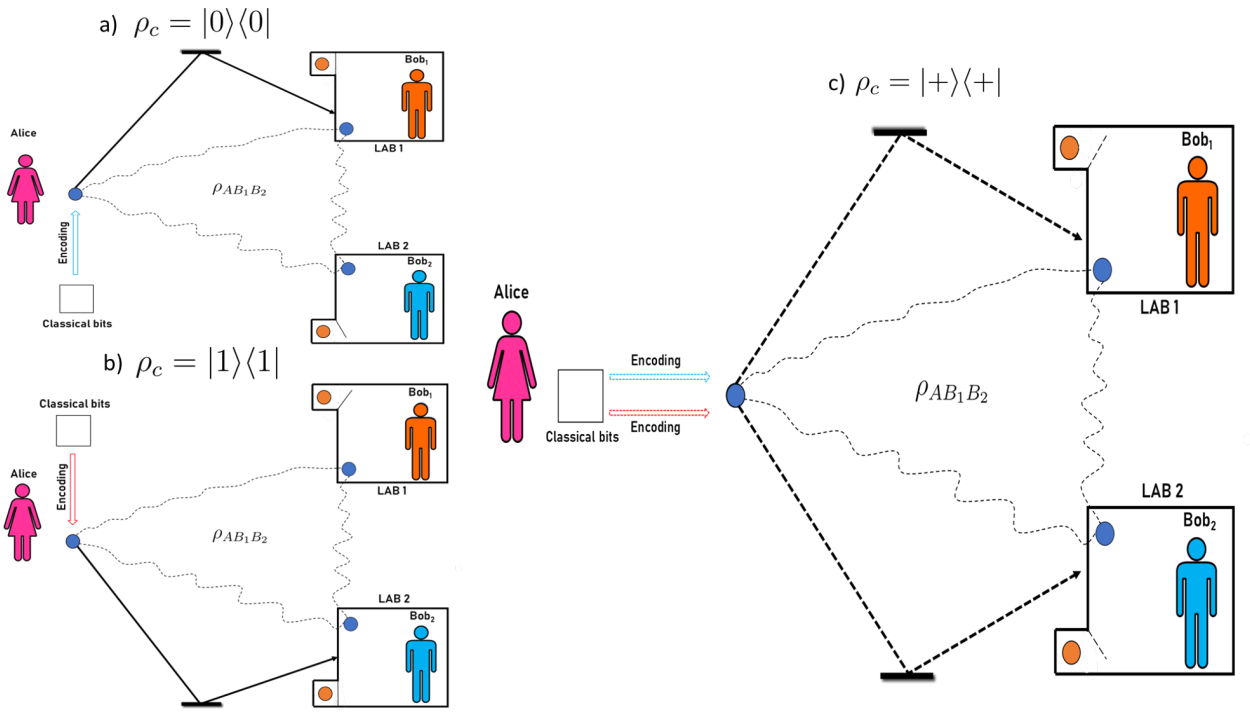

Figure 4.1: **a)** shows Process 1, where Alice encodes and routes her quantum system to lab 1, and the orange ball in lab 2 represents a fixed auxiliary state, $|0\rangle$. This is associated with the state $\rho_c = |0\rangle\langle 0|$. Similarly, **b)** shows Process 2, where Alice encodes and routes her system to lab 2 with the auxiliary state, $|0\rangle$, in lab 1. This is associated with the state $\rho_c = |1\rangle\langle 1|$. In **c)**, by setting $\rho_c = |+\rangle\langle +|$, a superposition of Process 1 and 2 is created where the encoding and routing are coherently controlled. Here, it is important to note that the measurement outcome of the control quantum system needs to be sent via a noiseless classical channel with limited capacity to the receivers.

The crux of our protocol lies in the fact that, after Alice coherently sends her part of the shared state to the two receivers, the two unitaries U^x and V^x present in the state $|\Psi_x\rangle$ act in different laboratories, L_1 and L_2 respectively. This suggests that the process of encoding and sending cannot be considered separately but are to be considered together as a whole. This procedure of encoding and sending is coherently controlled; therefore, unlike the standard dense coding protocol, Alice routing her share of state to laboratories L_1 and L_2 is non-classical and non-deterministic. Processes 1 and 2, separately, are identical (say, $U = V$) up to a trivial re-ordering, but this ordering becomes non-trivial when we create a superposition of those processes. The following analogy explains it better: In process 1, Alice shares a chocolate with Bob$_1$, and in process 2, Alice shares a chocolate with Bob$_2$. Both these processes are identical up to a trivial renaming of Bob$_1$ as Bob$_2$ and vice-versa. When one creates a superposition of processes 1 and 2, one cannot rename Bob$_1$ as Bob$_2$ (and

vice-versa), and here renaming becomes non-trivial.

The map W_x should be best thought of as an effective mathematical description—a "supermap"—that captures the joint evolution of the target (Alice's system and the receivers' subsystems, including the auxiliaries) and the control system. Since the structure of the unitary, W_x, is known to us, it defines our protocol. Then, for an arbitrary state $\rho_{B_1AB_2}$, including mixed ones, the ensemble possessed by the labs is $\mathcal{E} = \{p_X(x), \rho_x\}$, where

$$\rho_x = \mathrm{Tr}_c \left[\frac{(\mathcal{I}_t \otimes \Pi_+)(W_x(\rho_t \otimes \rho_c)W_x^\dagger)(\mathcal{I}_t \otimes \Pi_+)}{\mathrm{Tr}\left((\mathcal{I}_t \otimes \Pi_+)(W_x(\rho_t \otimes \rho_c)W_x^\dagger)\right)} \right] \tag{4.9}$$

where $\rho_t = \rho_{B_1AB_2} \otimes |0\rangle\langle 0|$ and $\Pi_+ = |+\rangle\langle +|$. The control is traced out because the receivers do not have access to it. It is important that the outcome of the measurement performed on the control qubit is classically communicated to the receivers. This one bit of information is transmitted through a noiseless classical channel. We will assume this noiseless classical channel has limited capacity, i.e., we can send one bit of information through it per quantum channel usage. We need to take this into account while comparing our protocol with the standard dense coding protocol.

Given the ensemble $\mathcal{E} = \{p_X(x), \rho_x\}$ with laboratories L_1 and L_2, we want to investigate how much encoded classical information is extractable if, in the first case, L_1 and L_2 can perform global measurements together, and in the second case, L_1 and L_2 are distant but can perform local operations and classical communication (LOCC) for decoding. Specifically, in the second case, one-way LOCC, denoted by $\texttt{LOCC}_1$, will be considered.

4.2.1 Global Decoding

When L_1 and L_2 are allowed to do global measurements to extract information from an encoded ensemble, $\mathcal{E}$, the accessible information is referred to as the globally accessible information of that particular ensemble and is denoted by $I_{acc}^{glo}(\mathcal{E})$. There is no general method to analytically calculate globally accessible information I_{acc}^{glo} [46, 38]. Still, there exists a useful upper bound to globally accessible information given by Holevo quantity $\chi(\mathcal{E})$, a function of the ensemble $\mathcal{E}$. For pure states, the Holevo quantity simplifies to $\chi(\mathcal{E}) = S(\rho_\mathcal{E})$ where $\rho_\mathcal{E}$ is the density matrix of ensemble $\mathcal{E}$, and more importantly, it is proven that the Holevo bound is asymptotically achievable [8], therefore, in our case, calculating the von-Neumann entropy is enough to obtain the globally accessible information. Maximising this

over all possible encodings allowed in our protocol gives DC capacity χ_{DC}. Particularly, in our case, the dense coding capacity with non-classical routing is given by

$$\begin{aligned}\chi_{NCR}^{glo} &= \max_{|\mathcal{X}|} \max_{U_2^x, V_2^x, p_X(x)} \chi(\mathcal{E}) \\ &= \max_{|\mathcal{X}|} \max_{U_2^x, V_2^x, p_X(x)} \left(S(\rho_{\mathcal{E}}) - \sum_{x \in \mathcal{X}} p_X(x) S(\rho_x) \right) \\ &= \max_{|\mathcal{X}|} \widetilde{\chi}_{NCR}^{glo}, \end{aligned} \tag{4.10}$$

where NCR denotes Non-Classical Routing and refers to our protocol.

Consider the state shared by Alice, Bob_1 and Bob_2 to be $\rho_{AB_1B_2}$. We parameterise the ensemble $\mathcal{E}$ by parametering single-qubit unitaries U^x and V^x (one of which is inclusive of global phase), the probabilities $p_X(x)$ and a numerical optimisation is carried out using the `trust-constr` optimisation, a method well suited for large-scale optimisations [15]. Let $|\mathcal{X}|$ denote the alphabet size where $\mathcal{X}$ is an alphabet of realisations x of the random variable X as letters. We will compare our protocol with the standard DC protocol by considering a few common classes of state.

Pure Entangled States

Let $\rho_{AB_1B_2} = |GHZ\rangle \langle GHZ|_{AB_1B_2}$ where $|GHZ\rangle_{AB_1B_2} = \frac{1}{\sqrt{2}}(|000\rangle + |111\rangle)$. An observation is made that in an optimal setting, there exists an encoding and a decoding scheme where, in an asymptotic limit, we have:

$$|\mathcal{X}| \leq 6 \Rightarrow \widetilde{\chi}_{NCR}^{glo} = \log |\mathcal{X}| \text{ bits} \tag{4.11}$$

$$|\mathcal{X}| \geq 6 \Rightarrow \chi_{NCR}^{glo} = \log 6 \approx 2.5849 \text{ bits} \tag{4.12}$$

Surprisingly, the maximum DC capacity of $\log 6$ is attainable even with a non-maximally entangled GHZ state. If $\rho_{AB_1B_2} = |gGHZ\rangle \langle gGHZ|_{AB_1B_2}$ where $|gGHZ\rangle_{AB_1B_2} = \cos(\theta/2)|000\rangle + \sin(\theta/2)|111\rangle$ is the generalised GHZ state but with the relative phase fixed to one, then we observe that $\chi_{NCR}^{glo} = \log 6$ bits is reachable for a wide range of $\theta \in [0.89, 2.25]$ about $\theta = \pi/2$ as seen in the FIG. 4.2.

Because our protocol makes use of a noiseless classical channel of limited capacity (one classical bit per quantum channel usage), during comparison, we need to give a boost of an extra bit to the standard dense coding capacity, making it useful for Alice to send three bits

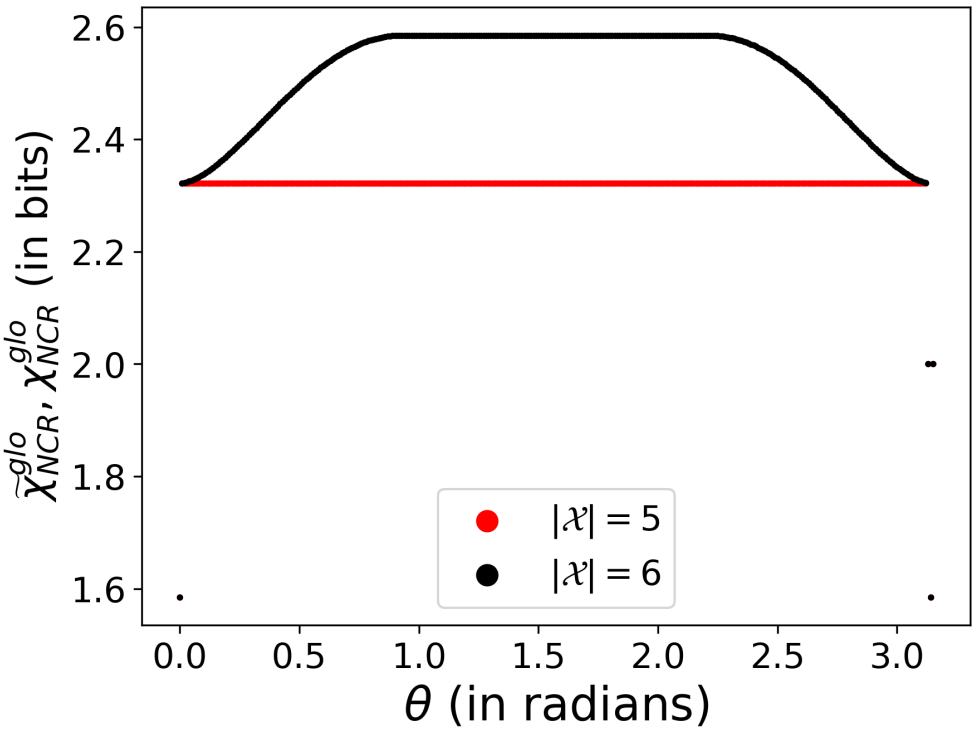

Figure 4.2: The black curve depicts the global dense coding capacity, χ^{glo}_{NCR}, along the vertical axis, as a function of the parameter θ of the generalised GHZ state, $|gGHZ\rangle$, along the horizontal axis. Intriguingly, we find that non-maximally entangled GHZ states also provide a dense coding capacity equal to $\log 6$. The red curve corresponds to the maximum globally extractable information, $\widetilde{\chi}^{glo}_{NCR}$, for an alphabet size $|\mathcal{X}| = 5$. In both cases, the capacities abruptly drop to $\log 3$ at values of θ equal to 0 and π.

of useful information, two bits from SDC and one bit from the noiseless classical channel. Clearly, in scenarios with maximally entangled states, a standard DC protocol with three bits is more useful than our DC protocol with $\log 6$ bits. However, two bits from SDC is possible only with a maximally entangled GHZ state, but our protocol has shown maximum "dense codeability" even with non-maximally entangled GHZ states; therefore, the tradeoff $\Delta = \chi^{glo}_{NCR} - (\chi_{SDC} + 1)$ is the quantity of interest, and $\Delta > 0$ implies an advantage in our protocol while $\Delta \leq 0$ implies the standard dense coding protocol to be more advantageous. As seen in FIG. 4.3, our protocol is better than the standard dense coding protocol for low-entangled GHZ states.

We can give a heuristic explanation as to why we can go above $\log 4$ bits. The argument follows like this: Any single-qubit unitary $U = e^{i\alpha}e^{-i\theta\frac{\hat{n}\cdot\vec{\sigma}}{2}}$ can be approximated as $U \approx (1+i\alpha)\mathcal{I}+\delta U$ where $\delta U \propto -i(\theta_x\sigma_x+\theta_y\sigma_y+\theta_z\sigma_z)$ where $n_i\theta = \theta_i$. Similarly, for $V = e^{i\beta}e^{-i\phi\frac{\hat{k}\cdot\vec{\sigma}}{2}}$,

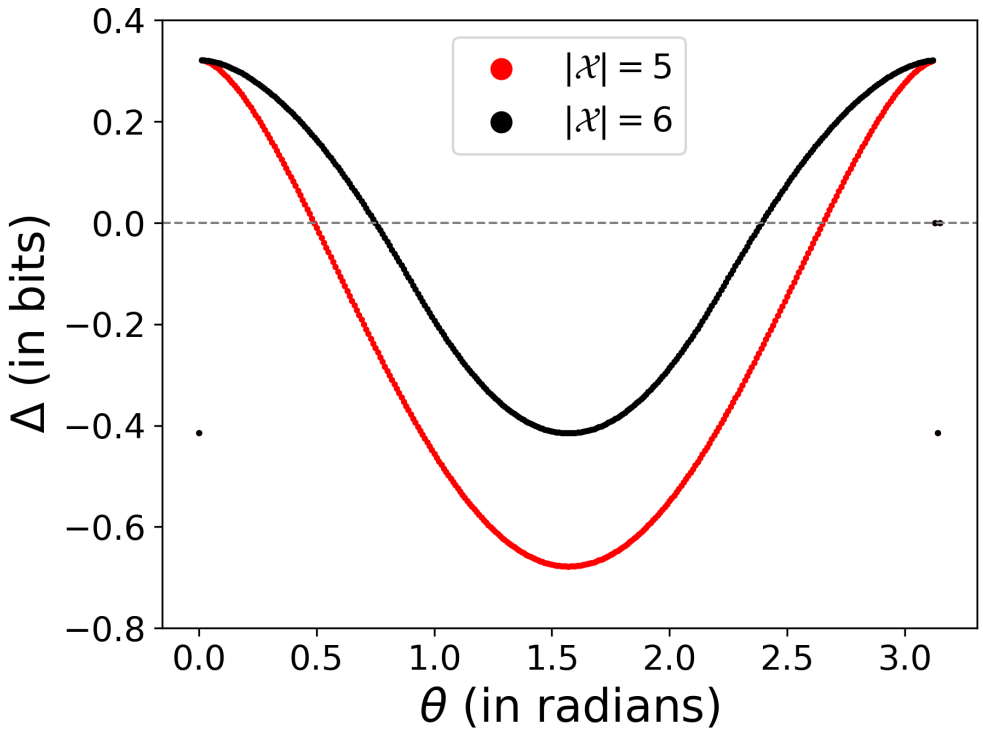

Figure 4.3: The figure of merit chosen for comparing our dense coding protocol with the standard one, given by $\Delta \equiv \chi_{NCR}^{glo} - (\chi_{SDC} + 1)$, is plotted along the vertical axis, as a function of θ of generalised GHZ along the horizontal axis. The black corresponds to our dense coding protocol with $|\mathcal{X}| = 6$, and the red corresponds to the same with $|\mathcal{X}| = 5$. For low entanglement regions, we find $\Delta > 0$, where our protocol shows an advantage over the standard one.

we have $V \approx (1 + i\beta)\mathcal{I} + \delta V$ where $\delta V \propto -i(\phi_x\sigma_x + \phi_y\sigma_y + \phi_z\sigma_z)$ where $k_i\phi = \phi_i$. Then, we have:

$$(\mathcal{I}\otimes U\otimes\mathcal{I}\otimes\mathcal{I})\,|GHZ\rangle\,|0\rangle + (\mathcal{I}\otimes\mathcal{I}\otimes\mathcal{I}\otimes V)\cdot \texttt{SWAP}_{2,4}\,|GHZ\rangle\,|0\rangle = |GHZ\rangle\,|0\rangle + \delta\,|\psi\rangle \quad (4.13)$$

The term $\delta\,|\psi\rangle$ is the infinitesimal change in the quantum state due to an infinitesimal unitary transformation and is given as:

$$\begin{aligned}\delta\,|\psi\rangle &= \big(\mathcal{I}\otimes(i\alpha\mathcal{I} + \delta U)\otimes\mathcal{I}\otimes\mathcal{I}\big)\,|GHZ\rangle\,|0\rangle + \delta\,|\psi\rangle \\ &= \big(\mathcal{I}\otimes\mathcal{I}\otimes\mathcal{I}\otimes(i\beta\mathcal{I} + \delta V)\big)\texttt{SWAP}_{2,4}\,|GHZ\rangle\,|0\rangle \quad (4.14)\end{aligned}$$

We can ignore the global phase by setting $\alpha = 0$. Expanding the expression above gives:

$$\delta|\psi\rangle = i(\beta - \theta_z + \phi_z)|0000\rangle + (\phi_y - i\phi_x)|0001\rangle + (\theta_y - i\theta_x)|0100\rangle + i\theta_z|1110\rangle \\ - ((\theta_y + \phi_y) + i(\theta_x + \phi_x))|1010\rangle + i(\phi_z + \beta)|1011\rangle \quad (4.15)$$

Varying each parameter infinitesimally, we see that $\delta|\psi\rangle$ steers towards certain directions. In particular, varying $\theta_x, \theta_y, \theta_z, \phi_x, \phi_y$ individually gives us five different unique directions but varying ϕ_z and β steers towards $i(|1011\rangle - |0000\rangle)$ and $i(|0000\rangle + |1011\rangle)$, respectively. These two directions are linearly dependent, so we have only one unique direction instead of two unique directions. Therefore, through an infinitesimal unitary transformation, our protocol allows six different linearly independent directions. This gives a lower bound on the number of orthogonal vectors possible. We mention it to be the lower bound because of the possibility of overlooking the global structure. Had we considered a unitary evolution of $|0\rangle \to |0\rangle + e^{i\phi}|1\rangle$, then it is clear that for an infinitesimal unitary transformation, the protocol allows only one linearly independent direction, but from inspection, we see $\phi = 0$ and $\phi = \pi$ give two vectors that are not just linearly independent but also mutually orthogonal. This is because of our restricted analysis of only the local structure, not the global one. Either way, evidence of six linearly independent directions implies at least more than four mutually orthogonal vectors, therefore explaining why we can go past two bits (which requires four mutually orthogonal states).

Unentangled Pure States

Let $\rho_{AB_1B_2} = |\psi\rangle\langle\psi|$ such that $|\psi\rangle_{AB_1B_2} \equiv |\phi\rangle_A \otimes |\Phi\rangle_{B_1B_2}$, that is, $|\psi\rangle_{AB_1B_2}$ is unentangled in the bipartition of the sender and receivers. An observation is made that in an optimal setting, there exists an encoding and a decoding scheme where, in the asymptotic limit, we have:

$$|\mathcal{X}| \leq 3 \Rightarrow \widetilde{\chi}_{NCR}^{glo} = \log|\mathcal{X}| \text{ bits} \quad (4.16)$$

$$|\mathcal{X}| \geq 3 \Rightarrow \chi_{NCR}^{glo} = \log 3 \approx 1.5849 \text{ bits} \quad (4.17)$$

In this scenario, $\chi_{SDC} = 1$ as $\rho_{AB_1B_2}$ is a pure product state, but our protocol gives $\chi_{DC}^{glo} = \log 3$, therefore $\Delta = \log\frac{3}{4} < 0$. Our protocol is not useful with unentangled pure states.

Maximally Mixed State

Let $\rho_{AB_1B_2} = \frac{1}{8}(\mathcal{I}_A \otimes \mathcal{I}_{B_1} \otimes \mathcal{I}_{B_2})$ where $\mathcal{I}$ is a 2×2 identity operator. We make some peculiar observations. In an optimal setting, there exists an encoding and a decoding scheme where,

in the asymptotic limit, we have:

$$|\mathcal{X}| \leq 2 \Rightarrow \widetilde{\chi}_{NCR}^{glo} = \log |\mathcal{X}| \tag{4.18}$$

$$|\mathcal{X}| \geq 3 \Rightarrow \chi_{NCR}^{glo} \approx 1.2539 \text{ bits} \tag{4.19}$$

For a maximally mixed state, $\chi_{SDC} = 0$, therefore $\Delta \approx 0.2539$. Our protocol is able to utilise a maximally mixed state for dense coding!

Completely Separable Mixed State

Consider the initial shared state to take the form of a completely separable mixed state,

$$\rho_{AB_1B_2} = \sum_{i=1}^{k} p_i \rho_A^i \otimes \rho_{B_1}^i \otimes \rho_{B_2}^i \tag{4.20}$$

where we take $\rho^i \equiv \frac{1}{2}(\mathcal{I} + \hat{n} \cdot \vec{\sigma})$, $\hat{n}$ is a unit vector, $\vec{\sigma}$ is the Pauli vector, and $\sum_i p_i = 1$.

We observe that, for $k = 2$ and in an optimal setting, there exists an encoding and a decoding scheme where, in the asymptotic limit, we have:

$$|\mathcal{X}| \leq 4 \Rightarrow \widetilde{\chi}_{NCR}^{glo} = \log |\mathcal{X}| \tag{4.21}$$

$$|\mathcal{X}| = 5 \Rightarrow \widetilde{\chi}_{NCR}^{glo} \approx \log 5 \tag{4.22}$$

The state $\rho_{B_1AB_2}$ and the encoding that achieves $\widetilde{\chi}_{NCR}^{glo} \approx \log 5$ is given in the appendix. It is numerically calculated that for this state, $\chi_{SDC} = 1$, therefore giving us $\Delta \approx \log 5/4 > 0$ bits. Our protocol demonstrates that classical correlation helps in a dense coding protocol!

Noisy GHZ and W

Consider the initial state shared to be noisy GHZ and W state, taking the form,

$$\rho_{AB_1B_2}^{GHZ} = p \left|GHZ\right\rangle \left\langle GHZ\right| + \left(\frac{1-p}{8}\right) \mathcal{I}_{AB_1B_2} \tag{4.23}$$

$$\rho_{AB_1B_2}^{W} = p \left|W\right\rangle \left\langle W\right| + \left(\frac{1-p}{8}\right) \mathcal{I}_{AB_1B_2} \tag{4.24}$$

where $|GHZ\rangle = \frac{1}{\sqrt{2}}(|000\rangle + |111\rangle)$ and $|W\rangle = \frac{1}{\sqrt{3}}(|100\rangle + |010\rangle + |001\rangle)$, and p is the 'visibility' of the noisy state.

In this case, the standard DC capacities for $\rho^{GHZ}_{AB_1B_2}$ and $\rho^{W}_{AB_1B_2}$ is fairly easy to calculate. Consider the noisy GHZ state $\rho^{GHZ}_{AB_1B_2}$. We create an encoded ensemble by applying unitaries $\{\mathcal{I}, \sigma_x, \sigma_z, \sigma_x\sigma_z\}$ with probability $p_X(x) = 1/4 \ \forall \ x \in \mathcal{X}$. Then,

- $\mathcal{I}$ term: $p\Big(\ |000\rangle\langle 000| + |000\rangle\langle 111| + |111\rangle\langle 000| + |111\rangle\langle 111| \ \Big) + \left(\frac{1-p}{8}\right)\mathcal{I}_3$

  Using the resolution of identity $\mathcal{I}_3$, through inspection it is clear that the eigenvalues are: $\left(\frac{1-p}{8}, 8\right)$ and $\left(\frac{1+7p}{8}, 1\right)$, where the first term inside the bracket is the eigenvalue and the second term is its multiplicity.

- σ_x term: $p\Big(\ |100\rangle\langle 100| + |100\rangle\langle 011| + |011\rangle\langle 100| + |011\rangle\langle 011| \ \Big) + \left(\frac{1-p}{8}\right)\mathcal{I}_3$

  Through inspection, it is clear that the eigenvalues are: $\left(\frac{1-p}{8}, 8\right)$ and $\left(\frac{1+7p}{8}, 1\right)$, where the first term inside the bracket is the eigenvalue and the second term is its multiplicity.

- σ_z term: $p\Big(\ |000\rangle\langle 000| - |000\rangle\langle 111| - |111\rangle\langle 000| + |111\rangle\langle 111| \ \Big) + \left(\frac{1-p}{8}\right)\mathcal{I}_3$

  Through inspection, it is clear that the eigenvalues are: $\left(\frac{1-p}{8}, 8\right)$ and $\left(\frac{1+7p}{8}, 1\right)$, where the first term inside the bracket is the eigenvalue and the second term is its multiplicity.

- $\sigma_x\sigma_z$ term: $p\Big(\ |100\rangle\langle 100| - |100\rangle\langle 011| - |011\rangle\langle 100| + |011\rangle\langle 011| \ \Big) + \left(\frac{1-p}{8}\right)\mathcal{I}_3$

  Through inspection, it is clear that the eigenvalues are: $\left(\frac{1-p}{8}, 8\right)$ and $\left(\frac{1+7p}{8}, 1\right)$, where the first term inside the bracket is the eigenvalue and the second term is its multiplicity.

- Overall encoded density matrix:

$$\frac{1}{4}\left[p\big(\ |000\rangle\langle 000| + |111\rangle\langle 111| + |100\rangle\langle 100| + |011\rangle\langle 011| \ \big) + \left(\frac{1-p}{8}\right)\mathcal{I}_3\right]$$

  The above expression is diagonal, and the eigenvalues are apparent: $\left(\frac{1-p}{8}, 4\right)$ and $\left(\frac{1+p}{8}, 4\right)$.

Then, the Holevo bound of the encoded ensemble is:

$$\begin{aligned}\chi^{GHZ}_{SDC} &= S(\rho_\mathcal{E}) - \sum_x p_X(x) S(\rho_x) = S(\rho_\mathcal{E}) - S(\rho_{x^*}) \\ &= \frac{1}{8}\big(3(1-p)\log(1-p) - 4(1+p)\log(1+p) + (1+7p)\log(1+7p)\big) \quad (4.25)\end{aligned}$$

Similarly, we can do the same for the noisy W state, $\rho^W_{AB_1B_2}$. I will list only the eigenvalues and their multiplicity for each term, as the expressions are huge. To $\rho^W_{AB_1B_2}$, Alice will apply the set of optimal unitaries for $d_A = 2$ with equal probabilities to give the following encoded ensemble:

- $\mathcal{I}$ term: The eigenvalues associated with this term are $\left(\frac{1-p}{8}, 7\right)$ and $\left(\frac{1+7p}{8}, 1\right)$
- σ_x term: The eigenvalues associated with this term are $\left(\frac{1-p}{8}, 7\right)$ and $\left(\frac{1+7p}{8}, 1\right)$
- σ_z term: The eigenvalues associated with this term are $\left(\frac{1-p}{8}, 7\right)$ and $\left(\frac{1+7p}{8}, 1\right)$
- $\sigma_x\sigma_z$ term: The eigenvalues associated with this term are $\left(\frac{1-p}{8}, 7\right)$ and $\left(\frac{1+7p}{8}, 1\right)$

Because the eigenvalues are symmetric in each term, the Holevo bound simplifies to:

$$\chi^{GHZ}_{SDC} = S(\rho_{\mathcal{E}}) - \sum_x p_X(x) S(\rho_x) = S(\rho_{\mathcal{E}}) - S(\rho_{x^*}) \tag{4.26}$$

where x^* is any particular realisation of the random variable X.

The eigenvalues and their multiplicity associated with the overall encoded ensemble are $\left(\frac{1-p}{8}, 4\right)$, $\left(\frac{3+p}{24}, 2\right)$ and $\left(\frac{3+5p}{24}, 2\right)$. Given the information of all these eigenvalues, the dense coding capacity of a noisy W state can be calculated to be

$$\chi^W_{SDC} = \frac{1}{24}\left(9(1-p)\log\left(\frac{1-p}{8}\right) - 2(3+p)\log\left(\frac{3+p}{24}\right) - 2(3+5p)\log\left(\frac{3+5p}{24}\right) + 3(1+7p)\log\left(\frac{1+7p}{8}\right)\right) \tag{4.27}$$

Unlike the noisy GHZ state, which can reach a maximum DC capacity of two bits, the noisy W reaches a maximum DC capacity of $\frac{1}{3}(1 + 3\log 3) \approx 1.918$ bits.

The plots of DC capacities of these states in the standard dense coding protocol and our DC protocol with non-classical routing are provided in FIG. 4.4. It can be seen that for our protocol, noisy GHZ and W have very similar performances, with noisy GHZ state taking a slight lead over noisy W state after $p = 0.6$, but we cannot be certain as this could be attributed to optimisation error. From FIG. 4.5, we see that our protocol performs better than the standard dense coding protocol for approximately $p < \frac{1}{2}$.

It is to be noted that in all of the above analyses, because there is no easy way to confirm if a non-linear numerical optimisation gives global extremum, the values above are, in fact,

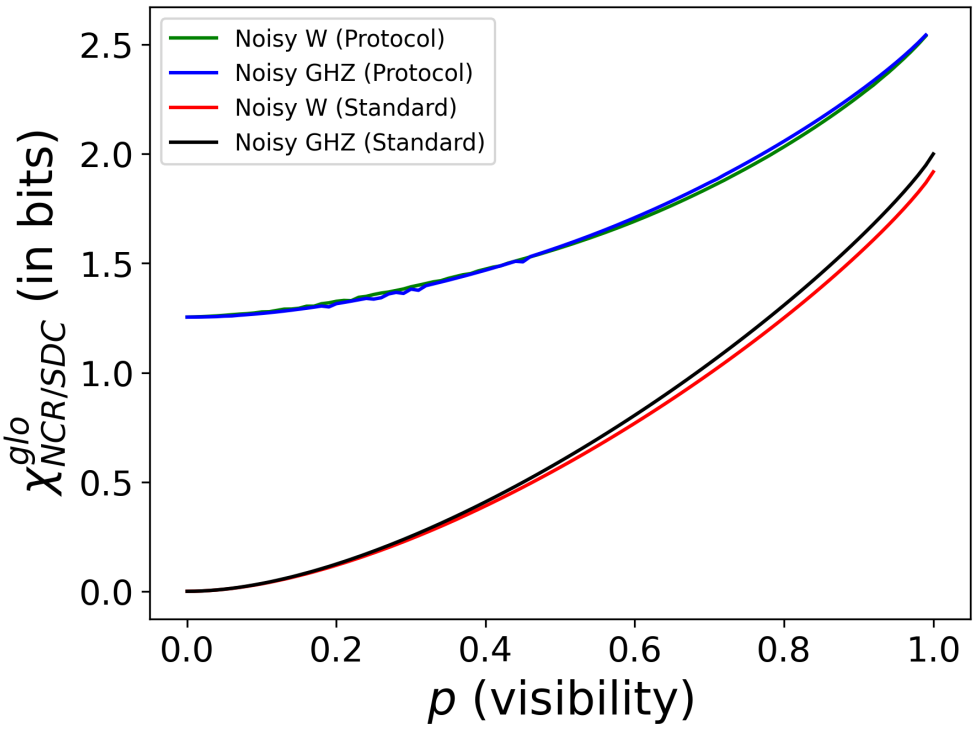

Figure 4.4: Global DC capacity, $\chi^{glo}_{NCR/SDC}$, as a function of visibility, p, associated with noisy GHZ and W states. As p approaches zero, the noisy GHZ and W states become more depolarised. 'Standard' refers to the standard dense coding protocol, and 'Protocol' refers to our dense coding protocol with non-classical routing.

lower bounds to χ^{glo}_{NCR}. We ascribe the reason as to why, in a few cases, we are able to go above two bits to the coherently controlled encoding and non-classical routing of states that allow the unitaries to effectively act on two different indices, thereby allowing us to access greater space of states through our protocol than those in standard dense coding protocols where Alice's unitaries act only on a single index. This greater space of states allows more "mixedness", allowing the von Neumann entropy to take values greater than $\log 4$.

4.2.2 LOCC Decoding

In the global decoding scenario, the receiver labs, L_1 and L_2, were assumed to be a single lab L as they were close enough to implement global measurements. A more realistic, practical, and non-trivial scenario would be to consider that the labs are far away from each other but have access to a stable classical channel and, therefore, can afford to perform LOCC-type measurements to extract information.

The maximal information that is extractable from a given bipartite ensemble restricted

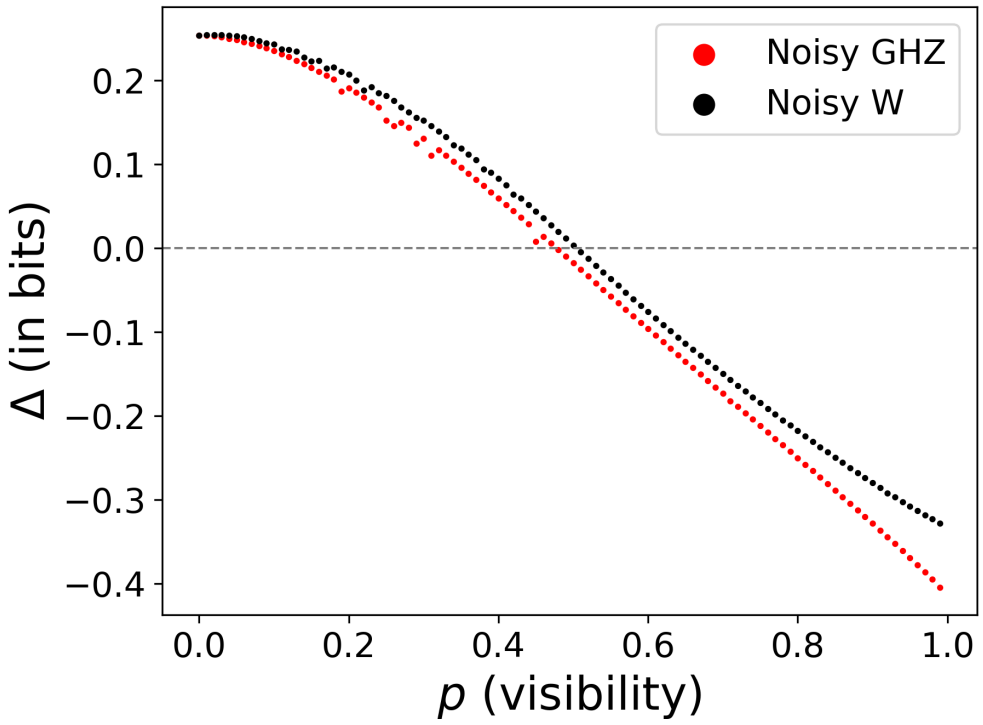

Figure 4.5: The figure of merit chosen for comparing our dense coding protocol with the standard one, given by $\Delta \equiv \chi^{glo}_{NCR} - (\chi_{SDC} + 1)$, is plotted along the vertical axis, as a function of visibility, p, of noisy W and GHZ states along the horizontal axis. The red curve corresponds to the noisy GHZ state, and the black curve corresponds to the noisy W state. Our protocol is advantageous as states get more depolarised.

to LOCC decoding strategies is referred to as the locally accessible information of that ensemble [3]. Like globally accessible information, there are no methods to calculate locally accessible information analytically, and it is even more complicated because the set of LOCC measurements has no tractable characterisation [14]. Nevertheless, an upper bound to locally accessible information was provided in [3], taking the form:

$$I^{LOCC}_{acc}(\mathcal{E}) \leq S(\rho_A) + S(\rho_B) - \max_{Z=A,B} \sum_{x \in \mathcal{X}} p_X(x) S(\rho^x_Z) \tag{4.28}$$

where $\mathcal{E} = \{p_X(x), \rho^x_{AB}\}$ is the bipartite ensemble, ρ_A and ρ_B are reductions of $\rho_{\mathcal{E}} = \sum_x p_X(x)\rho^x_{AB}$, and ρ^x_Z is a reduction of ρ^x_{AB}. A slightly stronger upper bound and a lower bound have also been looked into in [29, 44]. Unfortunately, as we discussed earlier, unlike the Holevo bound, this Holevo-like bound cannot be universally saturated for all ensembles, even in the asymptotic limit. However, some examples of ensembles have been found that do saturate it in $\mathbb{C}^n \otimes \mathbb{C}^n$ systems [3].

We will approach this problem by relaxing our problem to the class of one-way LOCC measurement protocols. We will refer to our one-way LOCC measurement protocol by $\texttt{LOCC}_1$. Before we get into the specifics of the protocol, it will be useful to write the mutual information in a more explicit form that we will use in numerical optimisation - for two random variables X and Y, we have

$$I(X;Y) = H(X) - H(X|Y) = -\sum_x p_X(x)\log p_X(x) + \sum_{x,y} p_{X,Y}(x,y)\log p_{X|Y}(x|y) \quad (4.29)$$

For $p_{X,Y}(x,y)$ and $p_{X|Y}(x|y)$, we can use Bayes theorem to obtain,

$$p_{X,Y}(x,y) = p_X(x)p_{Y|X}(y|x) = p_X(x)\text{tr}\{\Lambda_y\rho_x\} \quad (4.30)$$

$$p_{X|Y}(x|y) = \frac{p_{X,Y}(x,y)}{p_Y(y)} = \frac{p_{X,Y}(x,y)}{\sum_x p_{X,Y}(x,y)} = \frac{p_X(x)\text{tr}\{\Lambda_y\rho_x\}}{\sum_x p_X(x)\text{tr}\{\Lambda_y\rho_x\}} \quad (4.31)$$

Then, we express $I(X;Y)$ as

$$I(X;Y) = -\sum_x p_X(x)\log p_X(x) + \sum_{x,y} p_X(x)\text{tr}\{\Lambda_y\rho_x\}\log\left\{\frac{p_X(x)\text{tr}\{\Lambda_y\rho_x\}}{\sum_x p_X(x)\text{tr}\{\Lambda_y\rho_x\}}\right\} \quad (4.32)$$

The encoded ensemble $\mathcal{E} = \{p_X(x), \rho_x^{L_1L_2}\}$ is with labs L_1 and L_2. Without loss of generality, Bob_1 starts the $\texttt{LOCC}_1$ protocol by performing a POVM measurement $\mathcal{M} = \{\Lambda_{y_1}^{L_1}\}_{y_1\in\mathcal{Y}_1}$ on his subsystem (lab L_1) of the ensemble, obtains outcome $y_1^* \in \mathcal{Y}_1$ with probability $p_{Y_1}(y_1^*)$. Here, Y_1 is the information extracted by Bob_1 in the form of a random variable whose realisations y_1 are letters in the alphabet $\mathcal{Y}_1$. The outcome y_1^* is classically communicated to Bob_2 by Bob_1. Depending on this information received, Bob_2 performs the measurement $\mathcal{M}_2^{y_1^*} \equiv \{\Lambda_{y_2|y_1^*}^{L_2}\}_{y_2\in\mathcal{Y}_2}$ on the post-measurement ensemble and obtains outcome $y_2^* \in \mathcal{Y}_2$. Here, the measurement $\mathcal{M}_2^{y_1^*}$ is conditioned on the information y_1^* that Bob_1 sent to Bob_2. The $\texttt{LOCC}_1$ protocol ends here, and the total information extracted is given by $I(X;Y_1Y_2)$. From the chain rule of mutual information, as seen in (2.9), this becomes:

$$I(X;Y_1Y_2) = I(X;Y_1) + I(X;Y_2|Y_1) = I(X;Y_1) + \sum_{y_1} p_{Y_1}(y_1)I(X;Y_2|Y_1 = y_1) \quad (4.33)$$

where $\Lambda^{L_1} \equiv \Lambda^{L_1}\otimes\mathcal{I}^{L_2}$, $\Lambda^{L_2} \equiv \mathcal{I}^{L_1}\otimes\Lambda^{L_2}$, $p_{Y_1}(y_1) = \text{tr}\left\{\Lambda_{y_1}^{L_1}\rho_{\mathcal{E}}\right\}$ and $\rho_{\mathcal{E}}$ is the density operator of the encoded ensemble $\mathcal{E}$.

Assuming von Neumann-Lüder rule [9], once Bob_1's measurement yields outcome y_1^*, the

encoded ensemble $\mathcal{E} = \{p_X(x), \rho_x^{L_1L_2}\}$ collapses to the post-measurement ensemble $\mathcal{E}^{y_1^*} = \{p_{X|Y}(x|y_1^*), \rho_{x|y_1^*}^{L_1L_2}\}$. Because $p_{X|Y}(x|y) = \frac{p_X(x)p_{Y|X}(y|x)}{p_Y(y)}$, our post-measurement ensemble explicitly looks like:

$$\left\{ \frac{p_X(x)\mathrm{tr}\{\Lambda_{y_1^*}^{L_1}\rho_x^{L_1L_2}\}}{\sum_x p_X(x)\mathrm{tr}\{\Lambda_{y_1^*}^{L_1}\rho_x^{L_1L_2}\}}, \frac{\sqrt{\Lambda_{y_1^*}^{L_1}}\rho_x^{L_1L_2}\sqrt{\Lambda_{y_1^*}^{L_1}}}{\mathrm{tr}\{\Lambda_{y_1^*}^{L_1}\rho_x^{L_1L_2}\}} \right\} \tag{4.34}$$

The encoded ensemble $\mathcal{E}$ is referred to calculate $I(X;Y_1)$, and the post-measurement ensemble $\mathcal{E}^{y_1^*}$ is referred to calculate $I(X;Y_2|Y_1 = y_1^*)$. To ease numerical optimisation, we restrict the set of POVM measurements to rank-1 PVM measurements. This is done to reduce the number of parameters as well as the computational cost of evaluating the root of a POVM element. With projectors, we have $\sqrt{\Pi} = \Pi$ for all projective operators Π. The four-dimensional rank-1 PVM measurement set is given by $\{\Pi_i \equiv U|i\rangle\langle i|U^\dagger\}_{i=1}^4$ where $\{|i\rangle\}_i$ is the set of two-qubit basis states and U is an arbitrary two-qubit unitary operator taking the form:

$$U = (A \otimes B)U_d(C \otimes D) \tag{4.35}$$

where $A, B, C, D \in U(2)$, and U_d is a "non-local" unitary on $\mathbb{C}^2 \otimes \mathbb{C}^2$ given by,

$$U_d = \exp(-i[\alpha_x\sigma_x \otimes \sigma_x + \alpha_y\sigma_y \otimes \sigma_y + \alpha_z\sigma_z \otimes \sigma_z]) \tag{4.36}$$

where $\alpha_x, \alpha_y, \alpha_z \in \mathbb{R}$.

Using the `trust-constr` optimisation method available in Python's SciPy, we optimise over both the ensemble and rank-1 PVM $\texttt{LOCC}_1$ protocol together. Consider a generalised GHZ state, $|gGHZ\rangle$, where $|gGHZ\rangle = \cos(\theta/2)|000\rangle + \sin(\theta/2)|111\rangle$. We make an observation that there exists an encoding and a one-shot decoding scheme where

$$|\mathcal{X}| = 5 \Rightarrow I(X;Y_1Y_2) = 2.3215 \text{ bits} \Rightarrow I_{acc}^{LOCC_1} \geq 2.3215 \text{ bits} \tag{4.37}$$

This occurs when the generalised GHZ state has negligible but non-zero entanglement as $\theta \approx 0.01470$ and $\theta \approx 6.26848$, both around 0.01470 radians away from $\theta = 0$ and $\theta = 2\pi$, respectively. Interestingly, we also see that there exist one-shot $\texttt{LOCC}_1$ decoding protocols that saturate globally accessible information for $|\mathcal{X}| \leq 4$, i.e,

$$|\mathcal{X}| \leq 4 \Rightarrow I(X;Y_1Y_2) = \log|\mathcal{X}| = \widetilde{\chi}_{NCR/SDC}^{glo} \tag{4.38}$$

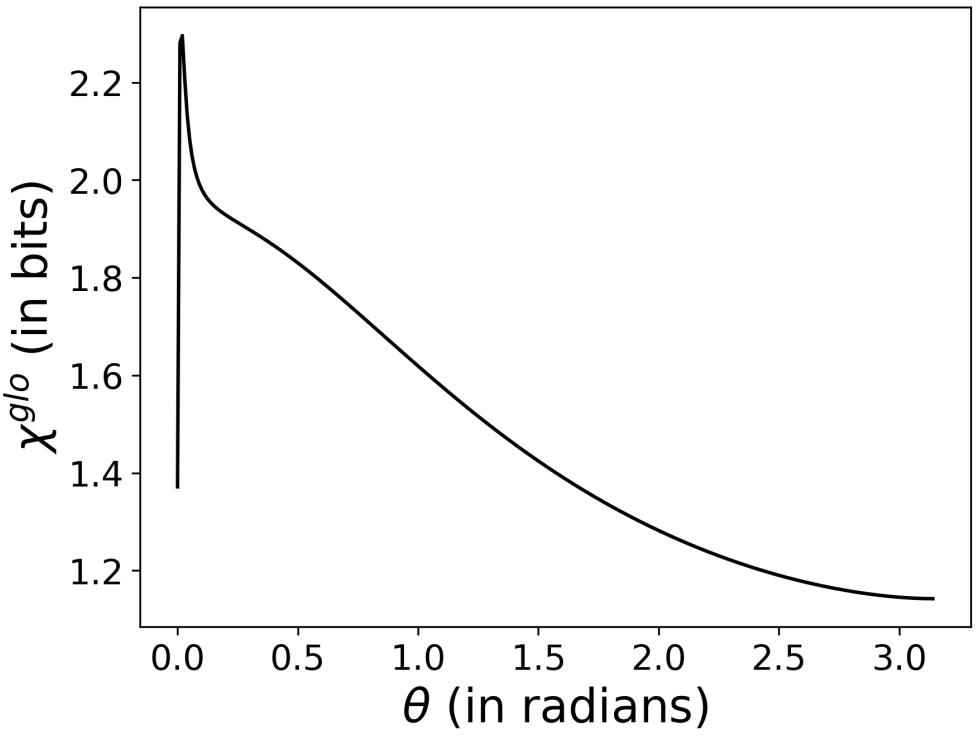

Figure 4.6: The curve depicts the global dense coding capacity, χ_{DC}^{glo}, along the vertical axis, as a function of the parameter θ of the generalised GHZ state, $|gGHZ\rangle$, along the horizontal axis. The ensemble under consideration is associated with $\texttt{LOCC}_1$ ensemble in (4.37). The global DC capacity shoots up immediately and then slowly decays.

By one-shot $\texttt{LOCC}_1$ decoding scheme, we mean that the sender has only sent a single string of the input quantum states $\rho^x_{L_1L_2}$. This is unlike the case seen when we saturate Holevo bound, as in that case, the decoding scheme asymptotically attains the bound if the sender could send long strings of the input quantum states.

To compare its performance with standard dense coding protocol in the LOCC decoding scenario, the equivalent scenario to be considered is Alice sends her encoded quantum system to Lab_1 with probability p and Lab_2 with probability $1-p$. Once sent, the amount of information extractable will be less than 2 bits because that is the globally accessible information. Let I_{acc}^{LOCC,L_1} and I_{acc}^{LOCC,L_2} be locally accessible information when Alice sends her system to lab_1 and lab_2, respectively. Then, the expected amount of extractable information in the standard dense coding scenario via LOCC measurements between the labs is:

$$\mathbb{E}(I_{acc}^{LOCC}) = pI_{acc}^{LOCC,L_1} + (1-p)I_{acc}^{LOCC,L_2} \leq p\chi_{SDC} + (1-p)\chi_{SDC} = \chi_{SDC} \tag{4.39}$$

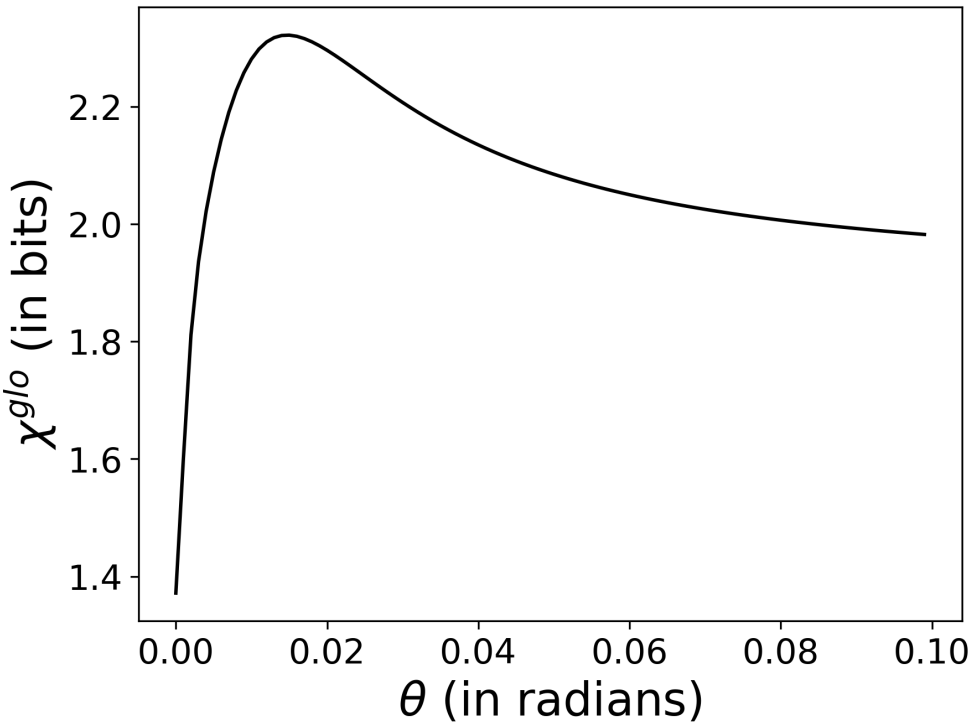

Figure 4.7: The curve depicts the global dense coding capacity, χ_{DC}^{glo}, along the vertical axis, as a function of the parameter θ of the generalised GHZ state, $|gGHZ\rangle$, along the horizontal axis. The ensemble under consideration is associated with $\texttt{LOCC}_1$ ensemble in 4.37. The global DC capacity shoots up immediately and then slowly decays. This is the zoomed-in plot around the maximum $\chi_{DC}^{glo} = 2.3218$.

If one uses a generalised GHZ with $\theta \approx 0.01470$, then $\chi_{SDC} \approx 1.0008$. Therefore, $\Delta \geq 2.3215 - (1.0008 + 1) = 0.3206 \Rightarrow \Delta \geq 0.3206$, implying an advantage even in our $\texttt{LOCC}_1$-based decoding protocol over the standard dense coding scenario with global decoding.

Interestingly, if we look at the global dense coding capacity associated with the $\texttt{LOCC}_1$ optimal ensemble, we see that the dense coding capacity shoots up very high and then decays, as seen in Fig. 4.6 and Fig. 4.7.

4.3 Multiple Receivers

Consider a single sender, Alice (A) and M receivers, Bobs ($B_1, \cdots, B_M$) where B_i resides in lab L_i, where each lab L_i has an auxiliary state $|0\rangle_{C_{B_i}}$. All $M+1$ parties share a $(M+1)$-qubit

generalised GHZ state:

$$|gGHZ_{M+1}\rangle_{AB_1\cdots B_M} = \cos\frac{\theta}{2}|0\rangle^{\otimes(M+1)} + e^{i\phi}\sin\frac{\theta}{2}|1\rangle^{\otimes(M+1)} \tag{4.40}$$

We can generalise our protocol to M receivers by creating a superposition of M processes. The control quantum system is an M-dimensional quantum state. For a given $x \in \mathcal{X}$, let $\{U_i^x\}_{i=1}^M$ be the set of unitaries to be multiplexed. The effective global unitary, in this case, that will be acting on the control and target is:

$$W_x = \sum_{i=1}^{M} (U_i^x)_{2i} \cdot \texttt{SWAP}_{2,2i} \otimes |i-1\rangle\langle i-1|_c \tag{4.41}$$

where $(U_j^x)_{2j}$ refers to single-qubit unitary $U_j^x \in \{U_i^x\}_{i=1}^M$ acting on the $2j^{th}$ index of a tensor product where all indices other than $2j^{th}$ index are identity operators, and $\texttt{SWAP}_{2,2i}$ is a $\texttt{SWAP}$ unitary acting on indices 2 and $2i$ ($\texttt{SWAP}_{2,2} = \mathcal{I}$).

This global unitary acts on the target-control joint state $W_x(\rho\otimes\rho_c)W_x^\dagger$ where $\rho_c = |+_d\rangle\langle+_d|$, $\rho = |\psi\rangle\langle\psi|$, $|+_d\rangle = \frac{1}{\sqrt{d}}\sum_{j=0}^{d-1}|j\rangle$ and $|\psi\rangle = |\psi\rangle_{B_1A:B_2C_{B_2}:\cdots:B_MC_{B_M}} \equiv |\psi\rangle_{L_1L_2\cdots L_M}$. After this unitary evolution, the control state is measured using the generalised Hadamard basis (for qudits), and the outcome corresponding to $|+_d\rangle\langle+_d|$ basis is post-selected. Then, the state now possessed at the receivers' end is:

$$|\Psi_x\rangle = \frac{1}{\sqrt{\langle\Psi_x|\Psi_x\rangle}}\left(\sum_{i=1}^{M}(U_i^x)_{2i}\cdot\texttt{SWAP}_{2,2i}\right)|\psi\rangle_{L_1L_2\cdots L_M} \tag{4.42}$$

As usual, $|\Psi_x\rangle$ is created with probability $p_X(x)$ to obtain the encoded ensemble $\mathcal{E} = \{p_X(x), \rho_x = |\Psi_x\rangle\langle\Psi_x|\}$. Since we know the form of W_x here, this protocol can be generalised to even mixed states, as we did earlier.

In a nutshell, using a M-dimensional quantum state as a control system, Alice coherently encodes and routes her quantum system to labs L_1 to L_M, in the process creating the encoded ensemble $\mathcal{E} = \{p_X(x), |\Psi_x\rangle\langle\Psi_x|\}$ possessed by all labs together.

4.3.1 Global Decoding

Entangled Pure States

Assuming the state shared by the sender and receivers is a $(M+1)$-qubit generalised GHZ state, numerical optimisation of χ_{NCR}^{glo} over all possible encodings is carried out, and some observations are made. In an optimal setting, there exists an encoding and a decoding scheme where, in the asymptotic limit, we have

$$|\mathcal{X}| \leq 2M+2 \Rightarrow \widetilde{\chi}_{NCR}^{glo} = \log|\mathcal{X}| \text{ bits} \tag{4.43}$$

$$|\mathcal{X}| \geq 2M+2 \Rightarrow \chi_{NCR}^{glo} = \log(2M+2) = 1+\log(M+1) \text{ bits} \tag{4.44}$$

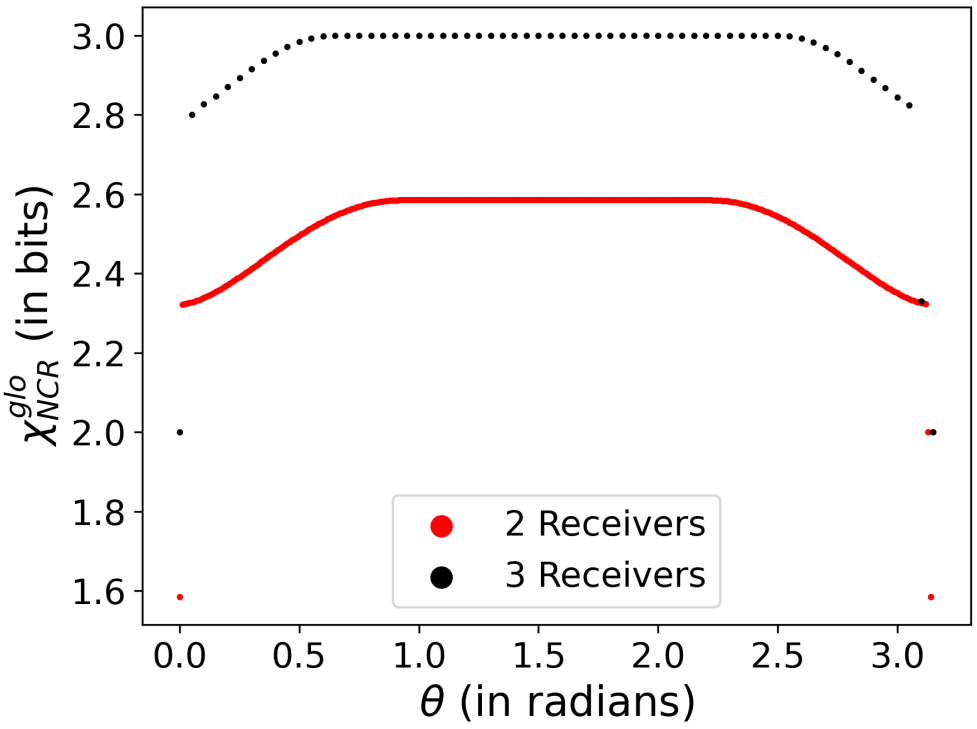

Figure 4.8: The black and red curves depict the global dense coding capacity, χ_{DC}^{glo}, along the vertical axis, as a function of the parameter θ of the generalised GHZ state $|gGHZ_4\rangle$ and $|gGHZ_3\rangle$, respectively. The DC capacity reaches the maximum for a greater range of θ in $M=3$ case than $M=2$ case.

Since the control is a d-dimensional quantum system, Alice must communicate $\log d$ bits of information about the communication outcome to the receivers. So, in this scenario, $\Delta \equiv \log(2M+2) - (\chi_{SDC} + \log M)$.

From Fig. 4.9, we see that $M = 3$ also provides an advantage but not better than the advantage seen in the $M = 2$ case. We suspect that, in this regard, $M = 2$ is the optimal distributed scenario.

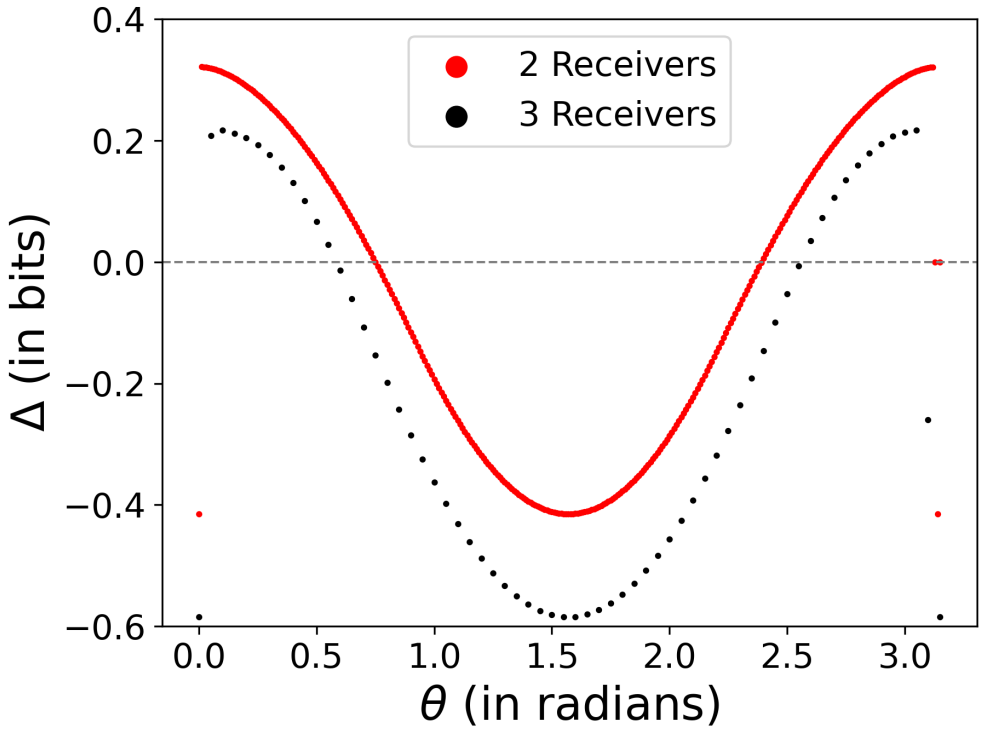

Figure 4.9: The figure of merit chosen for comparing our dense coding protocol with the standard one, given by $\Delta \equiv \chi_{NCR}^{glo} - (\chi_{SDC} + 1)$, is plotted along the vertical axis, as a function of θ of generalised GHZ $|gGHZ_{M+1}\rangle$ along the horizontal axis. The red curve corresponds to $M = 2$, and the black curve corresponds to $M = 3$. In terms of such a tradeoff, the two-receiver case performs better than the 3-receiver case.

Unentangled Pure States

If $\rho_{AB_1\cdots B_M}$ is a pure state, unentangled in the bipartition of $A : B_1 \cdots B_M$, then we observe that there exists an encoding and a decoding scheme where, in the asymptotic limit, we have,

$$|\mathcal{X}| < M + 1 \Rightarrow \widetilde{\chi}_{NCR}^{glo} = \log(|\mathcal{X}|) \text{ bits} \tag{4.45}$$

$$|\mathcal{X}| \geq M + 1 \Rightarrow \chi_{NCR}^{glo} = \log(M + 1) \text{ bits} \tag{4.46}$$

Therefore, $\Delta = \chi_{NCR}^{glo} - (\log M + \chi_{SDC}) = \log(M + 1) - \log M - 1 = \log(\frac{1}{2} + \frac{1}{2M}) \Rightarrow \Delta < 0 \; \forall \; M \in \mathbb{Z}^+$. As expected, our protocol is not advantageous with unentangled states even when $M > 2$.

We will not go into the LOCC decoding scenario in this context. For $M > 2$, the LOCC protocol would be more complicated than $\texttt{LOCC}_2$ between two parties. One way we can analyse this scenario is to pair up two parties as one and then consider the LOCC in their bipartition. However, analytical and even numerical analysis would be extremely hard in such scenarios. Further details regarding this are explained in [14].

Chapter 5

Conclusion

Dense coding has long been recognised as one of the cornerstone protocols in quantum communication, enabling the transmission of classical information at rates exceeding classical limits by leveraging quantum resources. While traditional approaches rely on quantum entanglement as a resource, recent advancements have explored the role of additional resources, such as coherent control and indefinite causal order, in enhancing communication protocols. Noting these, we make use of a coherent quantum system as a control in a dense coding protocol and find that the utilisation of a control quantum system helps provide dense coding capacity enhancement under global and $\texttt{LOCC}_1$ decoding strategies.

In the first half of this thesis, we explored key concepts from classical Shannon information theory, such as marginal entropy, conditional entropy, joint entropy, mutual information, and conditional mutual information, highlighting their connections to set theory and Venn diagrams. We then discussed various types of quantum measurements and introduced fundamental quantum information-theoretic terms, emphasizing their differences from classical Shannon theory. Building on these foundations, we reviewed existing literature on how classical information can be extracted from quantum ensembles through measurements. In particular, we examined global decoding scenarios, where receivers are close together, and LOCC (Local Operations and Classical Communication) decoding scenarios, where receivers are spatially separated but can communicate classically. With these prerequisites in place, we formally outlined a general dense coding protocol and its extensions to distributed settings, analyzing its performance under both global and LOCC decoding scenarios. Finally, we considered a scenario where a single sender, Alice, shares a generalized GHZ state with

two receivers, Bob_1 and Bob_2. We analytically derived the dense coding capacity in the standard protocol scenario and used it to compare it with our variant of dense coding protocol with non-classical routing.

In the second half of this thesis, we introduce a variant of the dense coding protocol that utilizes a control quantum system to coherently encode and route the sender's single-qubit system to Bob_1 and Bob_2. Specifically, we leverage a control quantum system to create a superposition of two dense coding scenarios, resulting in a protocol where Alice's encoding and her choice of routing her system to different labs are coherently governed by the state of the control system. In the global decoding scenario, we numerically maximize the Holevo quantity, $\chi(\mathcal{E})$, of an encoded ensemble, $\mathcal{E}$, over all possible encodings permitted by our protocol to determine the dense coding capacity. Since our protocol requires a noiseless classical channel to communicate the measurement outcome of the control quantum system to the receivers, we impose a constraint that this classical channel has limited capacity, allowing only one bit of information to be transmitted per quantum channel use. To ensure a fair comparison, we account for this additional classical resource in the standard dense coding scenario. To evaluate the advantage of our protocol over standard dense coding, we define the figure of merit as $\Delta \equiv \chi_{NCR}^{glo} - (\chi_{SDC} + 1)$, where $\Delta > 0$ indicates that our protocol outperforms the standard approach. For a certain set of weakly entangled GHZ states, a completely separable mixed state, and a maximally mixed state, we find $\Delta > 0$, demonstrating that our protocol outperforms the standard protocol. Additionally, we analyze noisy GHZ and W states, deriving their dense coding capacities in the standard scenario analytically and investigating their performance in the non-classical routing scenario numerically as a function of their visibility. Our findings indicate that in low-visibility regions, our protocol surpasses the standard dense coding protocol in performance.

In the LOCC decoding scenario, we simplify the problem by restricting the decoding measurements to a class of one-way LOCC measurements with rank-1 projective measurements, which we denoted as $\texttt{LOCC}_1$. Within this framework, we numerically optimize the mutual information between the sender's encoding and the receivers' decoding over all possible encoding strategies and $\texttt{LOCC}_1$ measurements. Our results show that for a nearly unentangled GHZ state, a specific one-shot $\texttt{LOCC}_1$ decoding strategy in our protocol can outperform the standard dense coding protocol even when the latter employs global decoding strategies, which are considered in the asymptotic limit, under the same nearly unentangled GHZ state.

We then extend our protocol from two receivers to M receivers, where Alice utilizes an M-

dimensional quantum system as a control to superpose M different processes. Focusing on the global decoding scenario, we observe that for a GHZ state, the dense coding capacity in our protocol increases monotonically with M. Specifically, we find that $\chi_{NCR}^{glo} = 1 + \log(M+1)$ for entangled states and $\chi_{NCR}^{glo} = \log(M+1)$ for unentangled states in the bipartition of senders to receivers. To fairly compare our protocol with the standard dense coding protocol, we account for the additional classical communication required by our scheme. Since we employ a noiseless classical channel, the figure of merit used for comparison is defined as $\Delta \equiv \chi_{NCR}^{glo} - (\chi_{SDC} + \log M)$. Our results indicate that for low-entangled GHZ states, our protocol outperforms the standard protocol. However, we also find that the $M = 2$ case generally performs better than $M = 3$. We attribute this to the fact that while χ_{NCR}^{glo} increases with M, the advantage gained is offset by the growing cost of the additional classical communication required to transmit the measurement outcome to the receivers.

Possible future directions include deriving analytical expressions for the dense coding capacity in both global and one-way LOCC decoding scenarios, which could provide deeper insights into the fundamental limits of our protocol. Additionally, further investigation is needed to understand the potentially active role of auxiliary systems in enhancing the protocol's performance and whether they contribute beyond merely serving as control systems. Another important avenue is to assess the experimental feasibility of our protocol by determining whether our variant of dense coding protocol can be physically implemented using current or near-future quantum technologies. This includes investigating practical methods for realizing the coherent control of encoding and routing, as well as identifying potential quantum systems and operations that can support the required superposition of dense coding processes.

Bibliography

[1] Alastair A Abbott, Julian Wechs, Dominic Horsman, Mehdi Mhalla, and Cyril Branciard. Communication through coherent control of quantum channels. *Quantum*, 4:333, 2020.

[2] Mateus Araújo, Adrien Feix, Fabio Costa, and Časlav Brukner. Quantum circuits cannot control unknown operations. *New Journal of Physics*, 16(9):093026, 2014.

[3] Piotr Badziag, Michał Horodecki, Aditi Sen, and Ujjwal Sen. Locally accessible information: How much can the parties gain by cooperating? *Physical Review Letters*, 91(11):117901, 2003.

[4] Julio T Barreiro, Tzu-Chieh Wei, and Paul G Kwiat. Beating the channel capacity limit for linear photonic superdense coding. *Nature physics*, 4(4):282–286, 2008.

[5] Charles H Bennett and Stephen J Wiesner. Communication via one-and two-particle operators on einstein-podolsky-rosen states. *Physical review letters*, 69(20):2881, 1992.

[6] Sugato Bose, Martin B Plenio, and Vlatko Vedral. Mixed state dense coding and its relation to entanglement measures. *Journal of Modern Optics*, 47(2-3):291–310, 2000.

[7] Dagmar Bruß, G Mauro D'Ariano, Maciej Lewenstein, Chiara Macchiavello, A Sen, and Ujjwal Sen. Distributed quantum dense coding. *Physical review letters*, 93(21):210501, 2004.

[8] Dagmar Bruß, Maciej Lewenstein, Aditi Sen, Ujjwal Sen, GIACOMO MAURO D'ARIANO, and Chiara Macchiavello. Dense coding with multipartite quantum states. *International Journal of Quantum Information*, 4(03):415–428, 2006.

[9] Paul Busch, Pekka J Lahti, and Peter Mittelstaedt. *The quantum theory of measurement*. Springer, 1996.

[10] Jose L Cereceda. Quantum dense coding using three qubits. *arXiv preprint quant-ph/0105096*, 2001.

[11] Giulio Chiribella, Manik Banik, Some Sankar Bhattacharya, Tamal Guha, Mir Alimuddin, Arup Roy, Sutapa Saha, Sristy Agrawal, and Guruprasad Kar. Indefinite causal order enables perfect quantum communication with zero capacity channels. *New Journal of Physics*, 23(3):033039, 2021.

[12] Giulio Chiribella, Giacomo Mauro D'Ariano, Paolo Perinotti, and Benoit Valiron. Quantum computations without definite causal structure. *Physical Review A—Atomic, Molecular, and Optical Physics*, 88(2):022318, 2013.

[13] Giulio Chiribella and Hlér Kristjánsson. Quantum shannon theory with superpositions of trajectories. *Proceedings of the Royal Society A*, 475(2225):20180903, 2019.

[14] Eric Chitambar, Debbie Leung, Laura Mančinska, Maris Ozols, and Andreas Winter. Everything you always wanted to know about locc (but were afraid to ask). *Communications in Mathematical Physics*, 328:303–326, 2014.

[15] Andrew R Conn, Nicholas IM Gould, and Philippe L Toint. *Trust region methods*. SIAM, 2000.

[16] Tamoghna Das, R Prabhu, Aditi Sen, and Ujjwal Sen. Distributed quantum dense coding with two receivers in noisy environments. *Physical Review A*, 92(5):052330, 2015.

[17] Aditi Sen De and Ujjwal Sen. Quantum advantage in communication networks. *arXiv preprint arXiv:1105.2412*, 2011.

[18] Emmanuel Desurvire. *Classical and quantum information theory: an introduction for the telecom scientist*. Cambridge university press, 2009.

[19] Daniel Ebler, Sina Salek, and Giulio Chiribella. Enhanced communication with the assistance of indefinite causal order. *Physical review letters*, 120(12):120502, 2018.

[20] Ximing Fang, Xiwen Zhu, Mang Feng, Xi'an Mao, and Fei Du. Experimental implementation of dense coding using nuclear magnetic resonance. *Physical Review A*, 61(2):022307, 2000.

[21] Nicolai Friis, Vedran Dunjko, Wolfgang Dür, and Hans J Briegel. Implementing quantum control for unknown subroutines. *Physical Review A*, 89(3):030303, 2014.

[22] Nicolas Gisin, Noah Linden, Serge Massar, and Sandu Popescu. Error filtration and entanglement purification for quantum communication. *Physical Review A—Atomic, Molecular, and Optical Physics*, 72(1):012338, 2005.

[23] Kaumudibikash Goswami, Y Cao, GA Paz-Silva, J Romero, and AG White. Communicating via ignorance: Increasing communication capacity via superposition of order. *arXiv preprint arXiv:1807.07383*, 2018.

[24] Kaumudibikash Goswami and Fabio Costa. Classical communication through quantum causal structures. *Physical Review A*, 103(4):042606, 2021.

[25] Kaumudibikash Goswami, Christina Giarmatzi, Michael Kewming, Fabio Costa, Cyril Branciard, Jacquiline Romero, and Andrew G White. Indefinite causal order in a quantum switch. *Physical review letters*, 121(9):090503, 2018.

[26] Yu Guo, Xiao-Min Hu, Zhi-Bo Hou, Huan Cao, Jin-Ming Cui, Bi-Heng Liu, Yun-Feng Huang, Chuan-Feng Li, Guang-Can Guo, and Giulio Chiribella. Experimental transmission of quantum information using a superposition of causal orders. *Physical review letters*, 124(3):030502, 2020.

[27] Tohya Hiroshima. Optimal dense coding with mixed state entanglement. *Journal of Physics A: Mathematical and General*, 34(35):6907, 2001.

[28] Alexander Semenovich Holevo. Bounds for the quantity of information transmitted by a quantum communication channel. *Problemy Peredachi Informatsii*, 9(3):3–11, 1973.

[29] Michał Horodecki, Jonathan Oppenheim, Aditi Sen, and Ujjwal Sen. Distillation protocols: Output entanglement and local mutual information. *Physical review letters*, 93(17):170503, 2004.

[30] Xiao-Min Hu, Yu Guo, Bi-Heng Liu, Yun-Feng Huang, Chuan-Feng Li, and Guang-Can Guo. Beating the channel capacity limit for superdense coding with entangled ququarts. *Science advances*, 4(7):eaat9304, 2018.

[31] Pratham Hullamballi, Aparajita Bhattacharyya, and Ujjwal Sen. Distributed quantum dense coding enhanced with non-classical routing. *arXiv preprint arXiv:2503.16122*, 2025.

[32] Jietai Jing, Jing Zhang, Ying Yan, Fagang Zhao, Changde Xie, and Kunchi Peng. Experimental demonstration of tripartite entanglement and controlled dense coding for continuous variables. *Physical review letters*, 90(16):167903, 2003.

[33] Ling-Jun Kong, Rui Liu, Zhou-Xiang Wang, Yu Si, Wen-Rong Qi, Shuang-Yin Huang, Chenghou Tu, Yongnan Li, Wei Hu, Fei Xu, et al. Complete orbital angular momentum bell-state measurement and superdense coding. *arXiv preprint arXiv:1709.03770*, 2017.

[34] Hlér Kristjánsson, Giulio Chiribella, Sina Salek, Daniel Ebler, and Matthew Wilson. Resource theories of communication. *New Journal of Physics*, 22(7):073014, 2020.

[35] Xiaoying Li, Qing Pan, Jietai Jing, Jing Zhang, Changde Xie, and Kunchi Peng. Quantum dense coding exploiting a bright einstein-podolsky-rosen beam. *Physical review letters*, 88(4):047904, 2002.

[36] X Shu Liu, Gui Lu Long, Dian Min Tong, and Feng Li. General scheme for superdense coding between multiparties. *Physical Review A*, 65(2):022304, 2002.

[37] Klaus Mattle, Harald Weinfurter, Paul G Kwiat, and Anton Zeilinger. Dense coding in experimental quantum communication. *Physical review letters*, 76(25):4656, 1996.

[38] John Preskill. Quantum shannon theory. *arXiv preprint arXiv:1604.07450*, 2016.

[39] Lorenzo M Procopio, Amir Moqanaki, Mateus Araújo, Fabio Costa, Irati Alonso Calafell, Emma G Dowd, Deny R Hamel, Lee A Rozema, Časlav Brukner, and Philip Walther. Experimental superposition of orders of quantum gates. *Nature communications*, 6(1):7913, 2015.

[40] Giulia Rubino, Lee A Rozema, Daniel Ebler, Hlér Kristjánsson, Sina Salek, Philippe Allard Guérin, Alastair A Abbott, Cyril Branciard, Časlav Brukner, Giulio Chiribella, et al. Experimental quantum communication enhancement by superposing trajectories. *Physical Review Research*, 3(1):013093, 2021.

[41] Giulia Rubino, Lee A Rozema, Adrien Feix, Mateus Araújo, Jonas M Zeuner, Lorenzo M Procopio, Časlav Brukner, and Philip Walther. Experimental verification of an indefinite causal order. *Science advances*, 3(3):e1602589, 2017.

[42] Giulia Rubino, Lee A Rozema, Francesco Massa, Mateus Araújo, Magdalena Zych, Časlav Brukner, and Philip Walther. Experimental entanglement of temporal order. *Quantum*, 6:621, 2022.

[43] T Schaetz, Murray D Barrett, Dietrich Leibfried, J Chiaverini, Joseph Britton, Wayne M Itano, John D Jost, Christopher Langer, and David J Wineland. Quantum dense coding with atomic qubits. *Physical review letters*, 93(4):040505, 2004.

[44] Aditi Sen, Ujjwal Sen, and Maciej Lewenstein. Distillation protocols that involve local distinguishing: Composing upper and lower bounds on locally accessible information. *Physical Review A—Atomic, Molecular, and Optical Physics*, 74(5):052332, 2006.

[45] Zahra Shadman, Hermann Kampermann, Chiara Macchiavello, and Dagmar Bruss. Optimal super dense coding over noisy quantum channels. *New Journal of Physics*, 12(7):073042, 2010.

[46] Jun Suzuki, Syed M Assad, and Berthold-Georg Englert. Accessible information about quantum states: An open optimization problem. In *Mathematics of Quantum Computation and Quantum Technology*, pages 327–366. Chapman and Hall/CRC, 2007.

[47] Márcio M Taddei, Jaime Cariñe, Daniel Martínez, Tania García, Nayda Guerrero, Alastair A Abbott, Mateus Araújo, Cyril Branciard, Esteban S Gómez, Stephen P Walborn, et al. Computational advantage from the quantum superposition of multiple temporal orders of photonic gates. *PRX Quantum*, 2(1):010320, 2021.

[48] Augustin Vanrietvelde and Giulio Chiribella. Universal control of quantum processes using sector-preserving channels. *arXiv preprint arXiv:2106.12463*, 2021.

[49] Daxiu Wei, Xiaodong Yang, Jun Luo, Xianping Sun, Xizhi Zeng, and Maili Liu. Nmr experimental implementation of three-parties quantum superdense coding. *Chinese Science Bulletin*, 49:423–426, 2004.

[50] Kejin Wei, Nora Tischler, Si-Ran Zhao, Yu-Huai Li, Juan Miguel Arrazola, Yang Liu, Weijun Zhang, Hao Li, Lixing You, Zhen Wang, et al. Experimental quantum switching for exponentially superior quantum communication complexity. *Physical review letters*, 122(12):120504, 2019.

[51] Mark M Wilde. *Quantum information theory*. Cambridge university press, 2013.

[52] Brian P Williams, Ronald J Sadlier, and Travis S Humble. Superdense coding over optical fiber links with complete bell-state measurements. *Physical review letters*, 118(5):050501, 2017.

[53] Mário Ziman and Vladimír Bužek. Correlation-assisted quantum communication. *Physical Review A*, 67(4):042321, 2003.